Stony Brook University

Polymers for Novel Applications: I. Hydrogel Implants for Post-Lumpectomy Patients and II. Cellulose Nanofibrous Composite Membrane for Heavy Metal Adsorption

A Thesis Presented

by

Si Hui Guan

to

The Graduate School

in Partial Fulfillment of the

Requirements

for the Degree of

Master of Science

in

Chemistry

Stony Brook University

May 2012

Stony Brook University

The Graduate School

Si Hui Guan

We, the thesis committee for the above candidate for the

Master of Science degree, hereby recommend

acceptance of this thesis.

Benjamin Chu– Thesis Advisor
Distinguished Professor
Department of Chemistry

Trevor Sears–Chair
Professor
Joint with Brookhaven National Laboratory
Department of Chemistry

Benjamin S. Hsiao– Third member
Professor and Chair
Department of Chemistry

This thesis is accepted by the Graduate School

Charles Taber
Interim Dean of the Graduate School

Abstract of the Thesis

Polymers for Novel Applications: I. Hydrogel Implants for Post-Lumpectomy Patients and II. Cellulose Nanofibrous Composite Membrane for Heavy Metal Adsorption

by

Si Hui Guan

Master of Science

in

Chemistry

Stony Brook University

2012

I. Breast cancer patients who have followed the lumpectomy procedure to take out the infected tissue will leave an empty space in their breasts. The aim of this study is to design and synthesize a novel Pluronics-based hydrogel that is radiation resistant, osmotic pressure balanced, radiological imaging friendly, while temporarily replicating the physical and mechanical properties of the native breast tissue. In order to produce a photo-cross-linkable hydrogel, Pluronics F127 was chemically modified from copolymer Poloxamer 407, by using diacrylates. The modified hydrogel, to our knowledge, is non-toxic and biocompatible to the human body. Furthermore, it can act as a scaffold to regenerate natural tissue in the presence of growth factors. In the process, the hydrogel will be designed to degrade slowly in order to accommodate the regenerated tissue as well as to maintain the shape of the breast. Therefore, this new hydrogel will be an innovative approach for breast reconstruction applications.

II. The heavy metal pollution problem is an environmental concern in developing and developed countries. The current study is designed for a novel microfiltration membrane consisting of cellulose nanofibers (CNF) and amino-modified cellulose nanofibers (mCNF), infused in an electrospun polyacrylonitrile (PAN) scaffold on a non-woven polyethylene terephthalate (PET) support, which can effectively remove a range of heavy metals from water. The high porosity, large surface area per unit volume and dense charges of the nanoscale-web structure can provide the resultant micro-filtration membrane with an ability to remove 159mg Pb (II) per gram CNF (0.766 mmol/g) and 71mg Cr (VI) per gram mCNF(1.36 mmol/g) by static adsorption. For dynamic adsorption, the CNF composite membrane is able to remove 259 mg/g (1.25 mmol/g) Pb (II), while the mCNF composite membrane is able to remove 100 mg/g (1.92 mmol/g) Cr (VI). Furthermore, the composite membrane can be recycled by utilizing a desorption cycle, which can remove 100 % of the adsorbed metal ions from the membrane. Therefore, a low cost, safe and effective pathway for heavy metal ion removal has been developed.

Table of Contents

List of Equations

List of Figures

List of Tables

Acknowledgments

I would like to express my deep gratitude and respect to my research advisors Professor Benjamin Chu and Professor Benjamin S. Hsiao for their invaluable advice, continuous patience, stimulating support and encouragement to my research. They are the ones I would admire and appreciate in all my life. Their strict attitude towards the scientific research deeply impressed me and will greatly influence my future career. I would also like to give my thanks to Professor Michael Hadjiargyrou, Dr Chirakkal V. Krishnan, Dr. Jonathan Chiu and my committee member Professor Trevor Sears for their help, suggestions and their encouragements on my way to the M.S. degree. I would like to acknowledge the helpful mentoring of Graduate student Mahati Elluru and Ran Wang. The synthesis procedure for diacrylated Pluronics F127 was carried out in collaboration with graduate student Mahati Elluru under the supervision of Dr Hongyang Ma. In collaboration with Mahati Elluru, we carry out the photoinitiator cytotoxicity test, Cell Titer Aqueous Nan-Radioactive Cell Proliferation Assay (MTS Assay) and biological evaluation of Pluronics based hydrogels for pre-adipocyte viability and growth using the same procedures, performed the experiments independently, and then compared the results for reproducibility and consistency. Special thanks should also be given to the Student Affairs Coordinator of the Chemistry Department – Katherine M. Hughes, who I bothered most in the past two years, for her great help with numerous issues. Many thanks to our current and previous group members Xiaowei Li, Xiao Wang, Zhe Wang, Rui Yang, Zhi Rui Mo, Ying Su, Justin Che, Yang Liu, Tsung Ming Yeh, Dr. Dufei Fang, Dr Hongyang Ma, Shigeyuki Toki. I thank them for their help in research or daily life, as well as their helpful discussions in my thesis writing. Finally, I would like to express my special appreciation to my parents and friends for their continuous understanding and support.

Chapter I

1. Introduction

1.1. Background and Significance

Breast cancer is the second most prevalent cancer in women in the United States, and the chance of developing invasive breast cancer at some time in a woman's life is just a little less than 12% [1]. American women are facing the daunting statistical fact that an estimated 207,090 new cases of invasive breast cancer were diagnosed in 2010, and about 54,010 new cases of carcinoma in non-invasive pre-cancer [1]. Furthermore, approximately 39,840 women died from breast cancer in 2010 alone [1]. From 2004-2008, the median age of women that had been diagnosed as having cancer of the breast was 61, and the age-adjusted incidence rate was 124 per 100,000 women per year [2]. There are over 2.5 million breast cancer survivors in the United States at this time [1]. Early diagnosis of breast cancer provide opportunity for the patients to undergo lumpectomy, which requires the removal of only the tumor and surrounding margins of tissue so that patients can maintain the original physical appearance of the breasts [3]. In order to reduce the risk of a local recurrence, radiation therapy typically follows as soon as possible after lumpectomy. Therefore, it is very important to develop an implant that can sustain numerous repeated doses of radiation, maintain the desired physical and mechanical properties, and provide little obstruction to X-ray imaging analysis.

1.2. History of Breast Reconstruction

Petrolatum injections, paraffin, organogen, bioplaxm and silicone implants are the common materials for breast reconstruction in today's market [4]. However, these materials are not ideal

since they may cause breast firmness, skin changes, pain, and chronic inflammation [4].Other breast reconstruction procedures, such as using muscle and skin grafts from other parts of the patient are not only expensive and strenuous for both the patient and the surgeon, but also have disappointing results, such as uneven breast sizes [5].

Hydrogels are materials that have been wildly used. They contain a three-dimensional network of polymer chains which can imbibe large amounts of water or biological fluids, and thus can resemble a biological tissue. Moreover, hydrogels have been shown to effectively serve as reconstructive biomaterials with the potential to act as scaffolds for tissue regeneration [6].

1.3. Properties of Pluronics Hydrogels

The Pluronics are symmetric tri-block copolymers that have been approved by the United States Food and Drug Administration for medical and pharmaceutical applications [7]. The Pluronics have a temperature-dependent hydrophobic polypropylene oxide (PPO) in the center block and two hydrophilic polyethylene oxide (PEO) end blocks[8] (Figure 1.1).

The amphiphilic properties enable Pluronics to be used as carriers to deliver drugs [9]. With increasing temperature and at temperatures above a critical micelle temperature, the hydrophobic PPO block begin to self-associate, while the two end hydrophilic PEO blocks remain hydrated [10, 11, 12]. Therefore, at low temperatures, Pluronics solutions form a clear viscous fluid. With increasing temperature, they can become semi-solidified hydrogels [13, 14]. Moreover, by modifying the periphery of the Pluronic micelles, the micelles can be polymerized by covalent cross-links through ultraviolet irradiation in the presence of a photo-initiator, thereby producing non-dissolving and chemically cross-linked modified Pluronics hydrogel networks (Figure 1.2).

Also, the Pluronics hydrogel has been found to be resistant to gamma irradiation by a prior study in our research group.

1.4. Specific Aims

There are three specific aims to this study. The first objective is to modify the ends of Pluronic F127 (general structure PEO_{99}-PPO_{69}-PEO_{99}, molecular weight 1.26 x 10^4Da), so that the modified polymers could be photo-cross-linked by UV irradiation, resulting in forming a more stable chemically cross-linked hydrogel that is also radiation resistant and radiological imaging friendly. Then, by performing rheological, swelling and degradation studies to determine the stability and the physical and mechanical properties of the hydrogel, we could tune the properties of the hydrogel to mimic the natural breast tissue. Lastly, the hydrogel was evaluated biologically with pre-adipocyte cells to test its potential for cell viability and growth, as the scaffold could be used to regenerate natural breast tissues without creating any undesirable immune response.

2. Experimental

2.1. Materials

Pluronics F127 was obtained from the chemical company BASF. N-Methyl-2-pyrrolidinone (NMP) [M_n = 99 g/mol, anhydrous, 99.5%], acryloyl chloride [M_n = 91 g /mol, solution density 1.119 g/mL], deuterated dimethyl sulfoxide (DMSO) [M_n = 78 g/mol, anhydrous, 99.9%], Poly(ethylene oxide) (PEG) [average M_n = 1500 Da, powder] and Dubecco's Modified Eagle's Medium [sterile filtered endotoxin test] were purchased from Sigma-Aldrich.

Spectra/Por®BioTech regenerated cellulose membranes were purchased from Spectrum labs. Photoinitiator 4-(2-hydroxyethoxy)phenyl-(2-hydroxy-2-propyl)ketone(Irgacure 2959) was obtained from Ciba Specialty Chemicals. Established cell line 3T3-L1 mouse embryonic fibroblast-adipocyte cells were obtained from the American Type Culture Collection. Dulbecco's Phosphate Buffered Saline 1X (DPBS) ([-] Calcium Chloride, [-] Magnesium Chloride) was purchased from Gibco.

2.2. Synthesis of Diacrylated Pluronics F127

10g of Pluronics F127 and 200 ml of NMP were transferred into a 500 ml round bottom flask. Under magnetic stirring at 1200 rpm, the mixture was heated at 80℃ until all the polymers were dissolved. In order to optimize the diacrylated modification, the solution was purged with nitrogen gas to remove any moisture. The end hydroxyl groups of Pluronics copolymers were diacrylated by a ten-fold molar excess of acryloyl chloride solution (Figure 1.3). 1.29 ml of Acryloyl chloride solution was mixed with 50 ml of NMP and added to the Pluronics solution in a drop-wise manner by using an addition funnel over a period of 1.5 hours. The reaction mixture was stirred at 1200 rpm for three days. In order to purify the reaction mixture, dialysis by using regenerated cellulose membranes (from Spectra/Por® BioTech, with 8 – 10kD molecular weight cut off) as performed. The external water of the dialysis tubings were renewed three to four times every day over a period of 4 days, so that all the small molecules, such as NMP and excess acryloyl chloride, were leached out, leaving the aqueous solution of diacrylated Pluronics inside the tubing. In order to obtain dried diacrylated Pluronics products, the diacrylated Pluronics solution was lyophilized by using the Millrock Benchtop Freeze-Dryer operating at a pressure

below 500 mT at -45℃ for 7 days. The products were weighed to calculate the yield and transferred into vials to be kept in the refrigerator at 4 ℃ for later experimental uses. It should be noted that much of the experimental work described below was performed under joint efforts with Mahati Elluru by using the same procedures but by carrying out the experiments independently. The results were then pooled to cross check the findings and reproducibility.

2.3. Proton Nuclear Magnetic Resonance Spectroscopy (^{1}H NMR) Test of Diacrylated Pluronics F127

The degree of acrylation of Pluronics polymers end groups was evaluated by ^{1}H NMR. 0.1 g of diacrylated product was transferred to a NMR tube, and an appropriate amount of DMSO was added. The solution was heated in a water bath until all the products were dissolved. There were 3 methyl protons from each PPO segment for a total of 69 PPO segments, and if the Pluronics polymer was completely diacrylated, there will be 3 acryl protons from each of two acrylated end groups. The degree of acrylation was evaluated by comparing the methyl protons peaks (~ 1.00 ppm) with the acryl protons peaks (~6.00 ppm).

2.4. Oscillatory Rheology Test of Pluronics Base Hydrogels

The chemical cross-linking of the copolymer network strengthened the hydrogel and provided it the essential mechanical properties to mimic the native breasts tissue. An Anton Paar Physica MCR 301 rheometer was utilized for evaluating the mechanical properties of the hydrogel. The storage modulus (G') and the loss modulus (G'') of the hydrogel were measured to find out the optimum UV irradiation time that could produce a hydrogel with a storage

modulus value similar to that of the native breasts tissue. The storage modulus represents the elastic portion of the hydrogel while the loss modulus represents the viscous portion. The conditions for the measurements was of cone and plate geometry with a 0.5 mm gap and an angular frequency ranging from 0.01 rad/s to 1 rad/s, oscillatory rotations of the bottom plate of the rheometer in a constant strain of 2% and at the body temperature of 37 ± 0.5 ℃. In order to find out the ability to producing the Pluronics based hydrogel with different mechanical properties, different compositions of the hydrogels were fabricated and different UV irradiation times with the same energy were performed on them. All the samples were limited to a concentration of 30% w/v polymer hydrogel. The compositions and the UV irradiation times were as following: diacrylated Pluronics F127 mixed with PEG 3000 Da in the ratio of 2:1 was UV irradiated for 30 minutes; diacrylated Pluronics F127 mixed with PEG 1500 Da in the ratio of 3:1 was UV irradiated for 30 minutes, and diacrylated Pluronics F127 mixed with PEG 1500 Da in the ratio of 2:1 was UV irradiated, respectively, for 7 minutes, 10 minutes, 25 minutes, and 30 minutes. The storage modulus values of all the samples were measured after 24 hours of the UV irradiation to ensure that the cross-linking reaction was completed.

2.5. Preparation of Pluronics based hydrogels

In order to increase the porosity, the 30% w/v polymer hydrogels were prepared by mixing diacrylated Pluronics F127 with unmodified PEG. According to prior tests, diacrylated Pluronics F127 mixed with PEG 1500 Da in the ratio of 2:1 was the optimum composition and 30 minutes of UV irradiation time gave the best mechanical properties of the cross-linked hydrogel. The photoinitiator Irgacure 2925 was used to initiate the UV induced photo-cross-linking reaction,

which covalently cross-linked the double bonds of the newly synthesized acryl groups at the ends of the diacrylated Pluronics F127. The composition of the hydrogel solution was 20% w/v of diacrylated Pluronics F127, 10% w/v of PEG-1500, 0.05% w/v of photoinitiator and 70% w/v of solvent (de-ionized water for mechanical study and tissue culture medium for cell study). The mixture was kept in the refrigerator until all the powders were dissolved and formed a viscous solution. According to different studies, corresponding amounts of gel solutions were transferred into glass vials or a 24-well plate. The XL-1500 Spectrolinker, operating at a wavelength of 365 nm, energy of 999,900 $\mu J/cm^2$, and an intensity of 5500 $\mu W/cm^2$, was utilized for performing the UV induced photo-cross-linking.

2.6. Swelling and Degradation of the Pluronics Base Hydrogel

A swelling study was performed to test the stability and degradation rate of the Pluronics Based hydrogel.1 mL of the hydrogel solution was transferred into a vial and UV irradiated for 30 minutes with an estimated energy of 999,900 $\mu J/cm^2$. The UV irradiated sample was capped and kept at room temperatures for one day in order to make sure that the cross-linking reaction was completed. The weight and the storage modulus of the cross-linked hydrogel at were measured after the cross-linking reaction was completed and before the hydrogel was immersed in PBS to swell, this was day 0. The sample was immersed in PBS in a petri dish and kept in an incubator at 37 ℃. The weight and the storage modulus of the hydrogel were measured at day 1, 2, 3, 4, 7, 9 and 10. The hydrogel was dried with a laboratory Kimwipe® before all the measurements. The PBS was discarded after all the measurements and new fresh PBS was added afterward.

2.7. Preparation of Pre-adipocyte Culture for Cell Studies

10% w/v Bovine calf serum and 1% w/v Peniallin-streptomycin were added into modified Eagle's Medium (DMEM) so that the medium was ready for cell culture use. All the chemicals, such as DMEM, Dulbecco's Phosphate Buffered Saline 1X (DPBS) and trypsin, were kept in a refrigerator before use. They were heated in a 37 ℃ water bath and sterilized under UV for 5 minutes before use. Cell line 3T3-L1 pre-adipocyte was separated into culture as the protocol from the American Type Culture Collection and was kept in an incubator at 37 ℃. When the cell culture reached the maximum number that occupied all the space at the bottom of the petri dish, it needed to be spread and the method was described as follows. The medium of the culture was aspirated and the cells were washed with 5 mL DPBS twice. 5 mL of trypsin was added and the petri dish was incubated at 37 ℃ for 5 minutes so that the cells left the bottom of the petri dish. In order to weaken the toxicity of the trypsin, 5 mL of the medium was added and mixed well with the trypsin. The cell solution was transferred into a centrifuge tube and centrifuged at 1000 rpm for 5 minutes, so that all the cells could be collected at the bottom of the tube. After aspiration of the top solution, the cells were re-suspended evenly in 3 to 4 mL of the medium. The cell solution was separated into couple petri dishes, and enough amount of the medium was added to each petri dish so that about 10 mL of the medium was present in each of them. All the newly prepared cell cultures were observed under the microscope to make sure that the cells were healthy, and evenly distributed in the petri dish. They were then kept in an incubator at 37 ℃. The medium was renewed every 2 to 3 days.

2.8. Photoinitiator Cytotoxicity Test

The cytotoxicity of the photoinitiator Irgacure 2959 was tested to make sure any excess of photoinitiator left in the cross-linked hydrogel would not have a negative effect on the per-adipocyte culture. 600,000 per-adipocyte were seeded in each well of a 24 well plate, and concentrations of 0.025%, 0.05%, and 0.075% of Irgacure 2959 de-ionized water solution were added on the cells. Cells treated with pure de-ionized water were acted as a control. Cell cultures were placed in an incubator at 37 ℃ for two days, and then the cells were stained with Trypan blue and the viable cells were counted using a hemocytometer (#1490 from Hausser Scientific).

2.9. Cell Titer Aqueous Nan-Radioactive Cell Proliferation Assay (MTS Assay)

In order to test the viability of the MTS Assay to be utilized to measure cell activity and cell growth, it was performed on only pre-adipocyte culture without any Pluronics based hydrogel. 9,000 per-adipocyte were seeded in the wells of a 24 well plate, and 200 μl of the medium was added on the cells in each well. The wells that contained only the medium with no cells were acting as controls. Before all the absorbance readings were taken, 40 μl MTS was added to each well and the well plate was kept in the dark and incubated for 30 minutes. The absorbance readings of day 0, 3, 6, 8 were measured by an ELISA 400 spectrophotometer at 490 nm.

2.10. Biological Evaluation of the Pluronics based Hydrogel for Pre-adipocyte Viability and Growth

1 ml of hydrogel solution and a total of 10 samples were transferred into vials and UV irradiated for 30 minutes. The UV irradiated samples were capped and kept at room temperature

for 1 day to complete the cross-linking reaction. The samples were sterilized under UV for 5 minutes before any cells were added onto them.52,500 pre-adipocyte were placed on top of each hydrogel sample, and the well plate was incubated at 37 ℃ for 45 minutes so that the cells could settle down onto the gel. 2 wells that contained only the pre-adipocyte culture without any hydrogel were acted as controls. 2 mL of the medium was added into each well after incubation, and the well plate was kept in an incubator at 37 ℃. Phase Contrast microscopy images of the pre-adipocyte culture with the hydrogel were taken on day 3.

3. Results and Discussion

3.1. Synthesis of Diacrylated Pluronics F127 and ^{1}H NMR Test

The diacrylated Pluronics product obtained from the lyophilizer was white in color and powder-like in form. ^{1}H NMR spectroscopy was performed, and the degree of acrylation was evaluated by comparing the methyl protons peaks (~1.00 ppm) with the acryl protons peaks (~6.00 ppm) (Figure 1.4). The value of the methyl proton peaks represented 207 methyl protons per molecule, while the value of acryl proton peaks represented the number of acryl protons presented in one modified Pluronics F127 molecule. The ^{1}H NMR results of all the diacrylated Pluronics F127 products indicated that overall 85% to 95% of the Pluronics F127 polymers were modified through acrylation. This modification was sufficient for the polymers to undergo UV induced photo-cross-linking and form a hydrogel with proper mechanical properties.

3.2. UV Induced Photo-cross-linking of Pluronics based Hydrogels

The Pluronics based hydrogel solutions were yellow colored if the solvent was de-ionized water and red color if the solvent was the tissue medium. The solutions were very viscous in both

cases. After UV induced photo-cross-linking was completed, the Pluronics based hydrogel became a chemical cross-linked gel which could retain its morphology.

3.3. Oscillatory Rheology Test of Pluronics based Hydrogels

Values of the storage modulus for Pluronics based hydrogels with different composition and different UV irradiation times were compared in this test (Figure 1.5). The results showed that as the UV irradiation time was increased, the storage modulus of the diacrylated Pluronics F127 mixed with PEG1500 in 2:1 ratio was increased, probably due to an increase in the degree of cross linking of the diacrylated Pluronics F127. Also, diacrylated Pluronics F127 mixed with PEG1500 in 2:1 ratio had a higher storage modulus value than it was mixed with PEG3000 in the same ratio, and diacrylated Pluronics F127 mixed with PEG1500 in 2:1 ratio was stronger than they were mixed in a 3:1 ratio. The size of the PEG polymers and the ratio of the polymers in the mixture could affect the micelle structure of the hydrogel solution. The hydrogel will swell in the body fluid and the uncross-linked polymers will be leached out gradually. Then, it will lose its mechanical property. The initial mechanical property of the hydrogel should be relatively strong so as to be comparable to that of the native breast tissue. An optimal composition of the copolymers hydrogel was found to be 30% w/v with 20% w/v diacrylated Pluronics F127 and 10% w/v PEG1500. The optimal UV irradiation time was 30 minutes with an estimated energy of 999,900 $\mu J/cm^2$. By varying the composition and UV irradiation time, hydrogels with different mechanical properties to mimic the native breast tissue of different patient could be produced.

3.4. Swelling and Degradation of Pluronics based Hydrogels

The maximum frequency experienced by an individual is about 50 Hz, and the storage modulus values of the actual adipocyte tissue at this frequency and with a strain of 1-5% was in

the range of 11,000 Pa to 40,000 Pa [16]. A swelling study was performed to make sure that the Pluronics based hydrogel could maintain its mechanical properties within the range of the native adipocyte tissue. The weight of the hydrogel was almost doubled during the first day of swelling, and the hydrogel reached an equilibrium value in about 10 days (Table 1.1). The increase in weight of the hydrogel was due to the absorption of PBS, once the hydrogel structure had enough ions to maintain its osmotic pressure in the PBS, it stopped taking additional solution and could maintain the weight at equilibrium. This change in dynamic equilibrium implied that once the hydrogel was transferred into the human body, it could take in the body fluid in order to maintain the osmotic pressure balance. Therefore, in order to achieve an osmotic pressure balance, it is very important to provide a charge balance for the hydrogel. The storage modulus of the hydrogel decreased to almost half of its value in the first day of swelling, and it reached an equilibrium value in about the next 10 days (Figure 1.6). This could be due to the leaching out of the uncross-linked polymers in the hydrogel and the absorption of a large amount of PBS in the swelling process. These two problems as a result of osmotic pressure in balance should be corrected by introducing appropriate charge in the hydrogel. Although the mechanical properties of the hydrogels were weakened during swelling, the initial and final storage modulus values were within the range of 40,000 Pa to 11,000 Pa, which indicated that the mechanical properties of the hydrogels could be adjusted to fabricate a suitable scaffold for the breast implant.

3.5. Photoinitiator Cytotoxicity Test

The cytotoxicity of the photoinitiator Irgacure 2959 was evaluated by the viability and growth of per-adipocyte (Figure 1.7). The number of cells was decreased in all the samples by a small amount in two days, but the remaining cells in each well were healthy. With excess amount

of cells being seeded in each well at the beginning, the cells were in close contacted with each other. This close contact, inhibited cell growth and resulted in cell death. Despite the number of cells being decreased in the first two days, the samples with different concentrations of the photoinitiator behaved almost the same as the control. The concentration of the photoinitiator in the cross-linked hydrogel was expected to be no more than 0.05%. The finding suggests that the amount of photoinitiator used to cross link the hydrogel will not make it toxic to the cells, and the amount photoinitiator that possible being leached form the hydrogel will not affect cell growth.

3.6. Cell Titer Aqueous Nan-Radioactive Cell Proliferation Assay (MTS Assay) on Pre-adipocyte Culture

The MTS Assay was performed on pre-adipocyte culture to make sure it was viable to test the activity and growth of cells. All the absorbance readings of the cells were subtracted by the readings of the controls. The results are shown in Figure 1.8. Viable cells constantly reduce the MTS salt into a tetrazolium compound through the mitochondria, forming a product that has a purple-black color [17]. Therefore, an increase of absorbance indicated an increase of the healthy cells number. The results show that the cell activity on day 0 was very low, due to the presence of a very little amount of cells being seeded in the wells. The increase of absorbance on day 3 indicated a large number on cells growth between day 1 and day 3. The similar absorbance on day 6 to day 8 indicated that the cells had stop growing. The results were the same as expected, i.e., the small number of cells at the beginning provides more space for cells growth for 3 days. However, starting on day 3, a large amount of cells occupied all the space in the well so that they were in close contact with each other and thus inhibited the cell growth. This study suggests that

the MTS Assay is viable for testing cell activity and cell growth. The MTS must be added into the well plate to react with the cells, and the cell activity and cell growth were judged by the absorbance of the cell solution. However, since the cells may grow into the hydrogel and the hydrogel will affect the absorbance reading, it is difficult to perform the biological evaluation of the hydrogel. A different method or a modified MTS Assay method should be used for testing the cell activity and cell growth in future experiments.

3.7. Biological Evaluation of Pluronics based Hydrogel for Pre-adipocyte Viability and Growth

Biological evaluation of the hydrogel with pre-adipocyte cells was intended to test its potential for cell viability and growth. A positive finding can suggest that it can act as a scaffold to regenerate natural tissue without undesirable immune response. Due to unexpected difficulties, the MTS assay was unable to be performed on this study, but the Phase Contrast microscopy images of the pre-adipocyte culture with the hydrogel were taken. The images showed that the pre-adipocyte were healthy and able to grow next to the hydrogel on day 3 (Figure 1.9). Although this study cannot prove that the hydrogel is suitable to act as a scaffold to regenerate the natural breast tissue, the images at least suggest that the hydrogel is stable enough to maintain its shape in the pre-adipocyte culture for at least three days. This study also proved that the hydrogel as well as the chemicals being leached out, which were the 10%w/v PEG-1500, 0.05% w/v photoinitiator and a small amount of uncross-linked diacrylated Pluronics F127, were non-toxic to the pre-adipocyte, and the pre-adipocyte were viable and able to grow normally in the present of the hydrogel.

4. Conclusion

In this study, diacrylated Pluronics F127 copolymer was successfully synthesized, and the chemical cross-linked Pluronics based hydrogel was produced. The hydrogel is radiation resistant, radiological imaging friendly and can be fabricated in any desired shape and size. It is viable to be considered a possible scaffold for breast reconstruction for the breast cancer patient who has undergone lumpectomy.

The oscillatory rheology test showed that by varying the composition and the UV irradiation time, hydrogels with different mechanical properties to mimic the native breast tissue of different patient could be fabricated. The swelling study showed that the hydrogel was able to maintain its properties while in contact with the body fluid for a period of at least 10 days. In practice, the hydrogel should maintain its properties until the tissue was being regenerated. Therefore, a range of different degradation rate could be useful. The mechanical properties of the hydrogel can be altered by changing the hydrogel composition and the UV irradiation time. Furthermore, the hydrogel passed the preliminary phase of biological evaluation, indicating that its components were not toxic to the pre-adipocyte. The Pluronics-based hydrogel has the potential to serve as a space-filling scaffold for breast reconstruction and tissue regeneration.

Future research will be focus on the degradation of the hydrogel and the ability of the hydrogel to act as a scaffold to facilitate the growth of pre-adipocyte, so as to reach the goal of tissue regeneration. By varying the composition and UV irradiation time, not only different mechanical properties, but also different degradation rates of hydrogel could be achieved. The degradation rate of the hydrogel should be similar to the growth rate of the pre-adipocyte cells so that the space of the hydrogel would be replaced by newly generated tissues and the original

shape of the breast could be conserved. The surface of the hydrogel could be coated with fibronectin so that the pre-adipocyte will be more likely to settle down on the hydrogel and proliferate on it. The number of pores and the pore size of the hydrogel are very important for cells growth. The proper size and connectivity of the pores are essential for pre-adipocyte growth. Moreover, if time is available, the cell study would have been performed for a longer period of time to better confirm the ability of the hydrogel serving as a scaffold for tissue regeneration. The swelling study should also include measurements on the volume changes of the hydrogel. Cell differentiation ability of the hydrogel is another important study needed to be performed. Capillary vessel must be regenerated at the same time as the breast tissue so that there will be enough nutrition to be delivered to the breast tissue, which is essential for cell viability and growth. Overall, the successful synthesis of the Pluronics based hydrogel may produce a novel material for tissue regeneration applications.

References

1. American Cancer Society (2011). What are the key statistics about breast cancer. American Cancer Society, Inc.
2. National Cancer Institute (2011). Surveillance Epidemiology and End Results Stat Fact Sheets: Breast. Surveillance Research Program. Retrieved from http://www.cancer.gov.
3. Waljee JF, Hu ES, Ubel PA, Smith DM, Newman LA, Alderman AK. (2008). Effect of esthetic outcome after breast-conserving surgery on psychosocial functioning and quality of life. *Journal of Clinical Oncology, 26,* 3331-3337.
4. Marotta, J.S., Widenhous, C.W., Habal, M. B., & Goldberg, E. P. (1999). Silicon gel breast implant failure and frequency of additional surgeries: Analysis of 35 studies reporting examination of more than 8000 explants. *Journal of Biomedical Materials Research 48*(3), 354-364.
5. Kroll, S., & Baldwin, B. (1992). A comparison of outcomes using three different methods of breast reconstruction. *Plastic and Reconstructive Surgery: Journal of the American Society of Plastic Surgeons, 90*(3), 455-462.
6. Drury, J. L., & Mooney, D. J. (2003). Hydrogels for tissue engineering: Scaffold design variables and applications. *Biomaterials, 24,* 4337-4351.
7. Croy, S. R., & Kwon, G. S. (2004). The effects of Pluronics block copolymers on the aggregation state of nystatin. *Journal of Controlled Release, 95,* 161-171.
8. Wu, C., Chu, B., Schneider, D.K., &Graziano, V. (1997). Characterization of the PEO-PPO-PEO triblock copolymer and its application as a separation medium in capillary electrophoresis. *Macromolecules, 30,* 4574-4583.
9. Batrakova, E. V., & Kabanov, A. V. (2008). Pluronics block copolymers: Evolution of drug delivery concept form inter nanocarriers to biological response modifiers. *Journal of Controlled Release, 130*(2), 98-106.
10. Chu, B. (1995). Structure and dynamics of block copolymer colloids. *Langmuir, 11,* 414-421.
11. Wu, G., Zhou, Z., Chu, B. (1993). Water-induced micelle formation of block copoly(oxyethylene-oxypropylene-oxyethylene) in o-xylene. *Macromolecules, 26*(8), 2117-2125.
12. Chu, B., Liu, T., Wu, C., Zhou, Z., Nace, V. M. (1997). Structures and properties of block copolymers in solution. *Macromolecular Symposia, 1,* 221-227.
13. Kabanov, A. V., Nazatova, I. R., Astafieva, I. V., Batrakova, E. V., Alakhov, V. Y., Yarolavov, A. A., Kabanov, V.A. (1995). Micelle formation and solubilization of fluorescent probes in poly (oxyethylene-b-oxypropylene-b-oxyethylene) solutions. *Macromolecules, 28,* 2303-2314.
14. Wu, C., Liu, T., Chu, B. (1998). A new separation medium for DNA capillary electrophoresis: self-assembly behavior of Pluronicpolyol $E_{99}P_{69}E_{99}$ in 1X TBE buffer. *Journal of Non-Crystalline Solids, 235-237,* 605-611.
15. Lee, J. B., Yoon, J. J., Lee, D. S., & Park, T. G. (2004). Photo-crosslinkable, thermo-sensitive and biodegradable Pluronics hydrogels for sustained release of protein. *Journal of Biomaterials Science, 15*(12), 1571-1583.
16. Patel, P. N., Smith, C. K., & Patrick, Jr., C. W. (2005). Rheological and recovery properties of poly(ethylene glycol) diacrylate hydrogels and human adipocyte tissue. *Journal of Biomedical Materials Research, 73*(3), 313-319.

17. Cory, A. H., Owen, T. C., Barltrop, J. A., & Cory, J. G. (1991). Use of an aqueous soluble tetrazolium/formazan assay for cell growth assays in culture. *Cancer Communications, 3*(7), 208-212.

Appendices

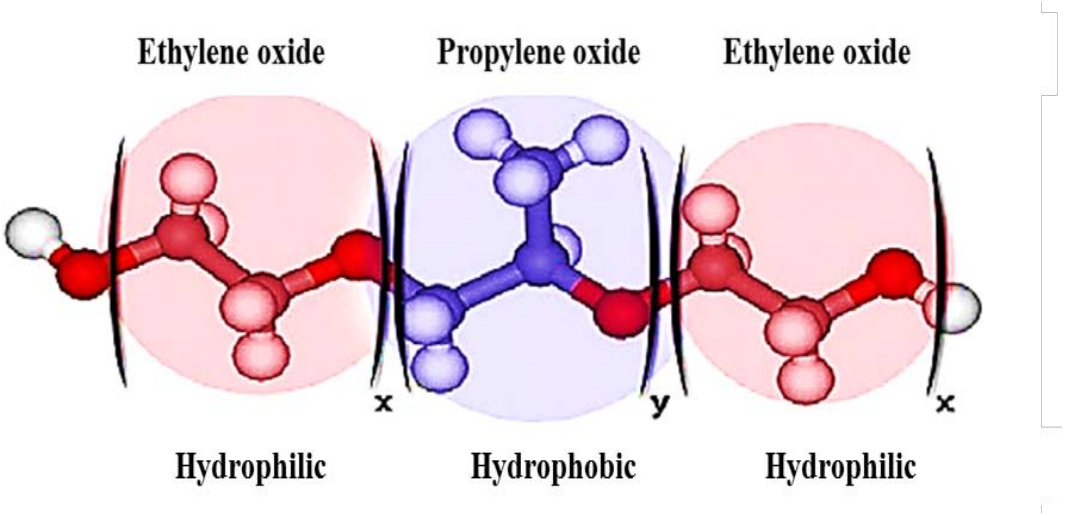

Figure 1.1: Pluronic tri-block copolymer molecule, x represents the number of PEO groups, y represents the number of PPO groups [9].

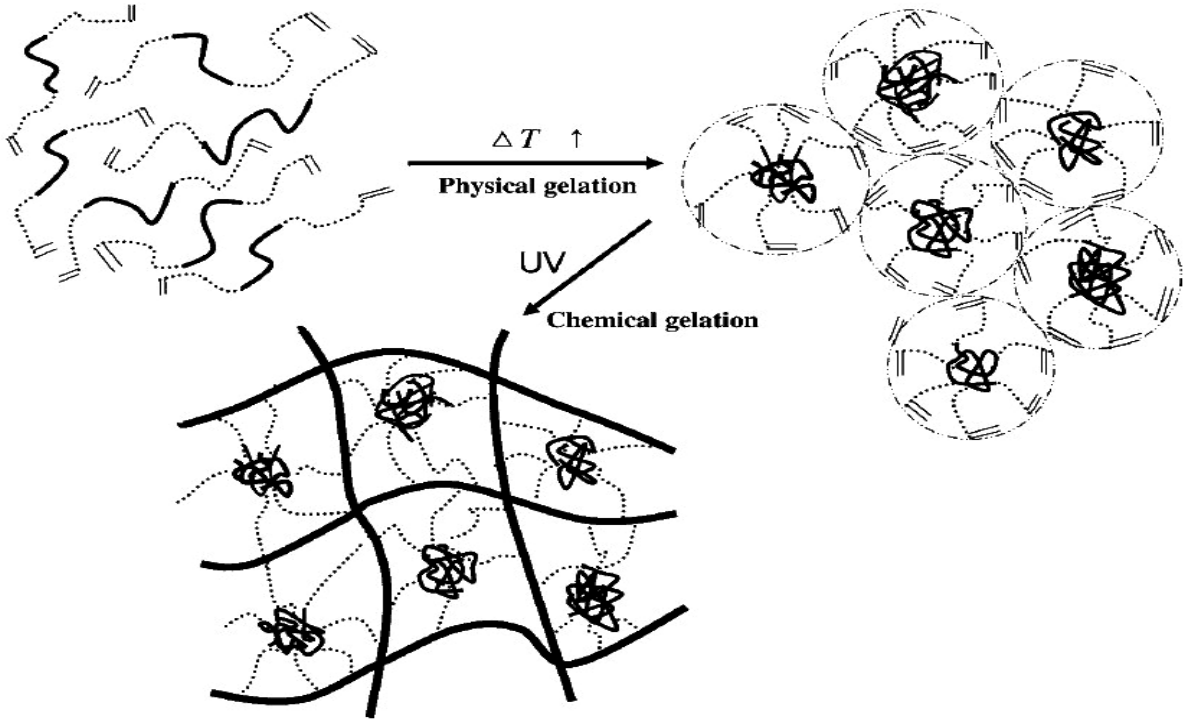

Figure 1.2: Physical gelation transition and UV-induced photo-cross-linking of diacrylated Pluronics tri-block copolymers. Pluronics tri-block copolymers are assumed to be in a closely packed state prior to photo-polymerization [15].

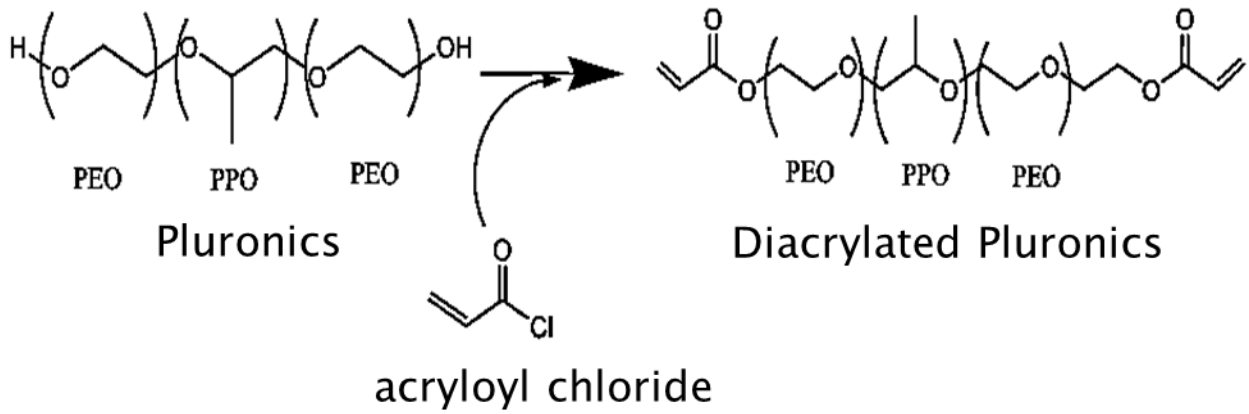

Figure 1.3: Diacrylated modification of Pluronics polymer.

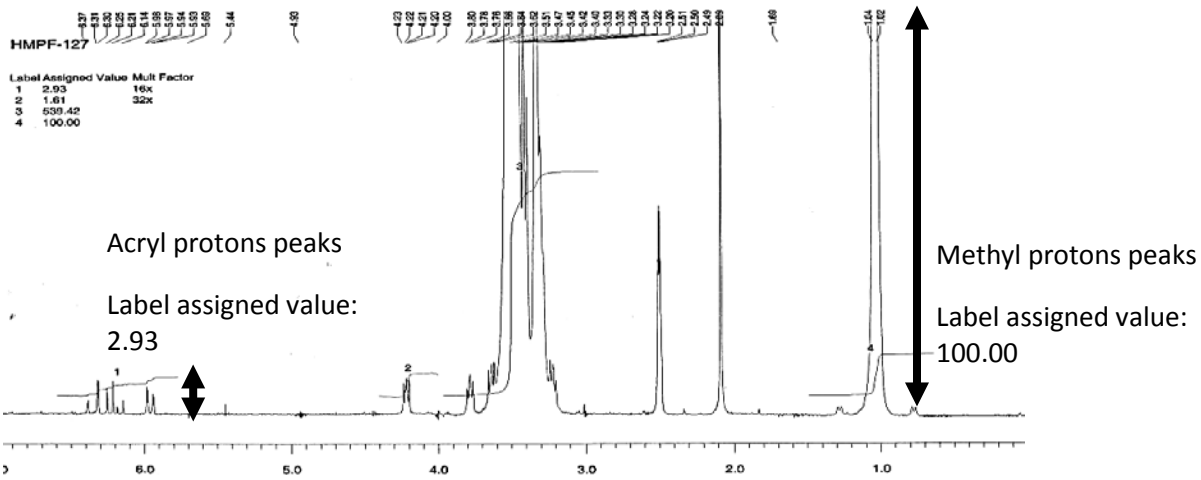

Figure 1.4: ^{1}H NMR spectrum confirming degree of diacrylation of the Pluronics F127 through comparison of acryl protons peaks (`~6.00 ppm) and methyl protons peaks (~1.00ppm). The acryl protons peaks shown here were amplified 16 times.

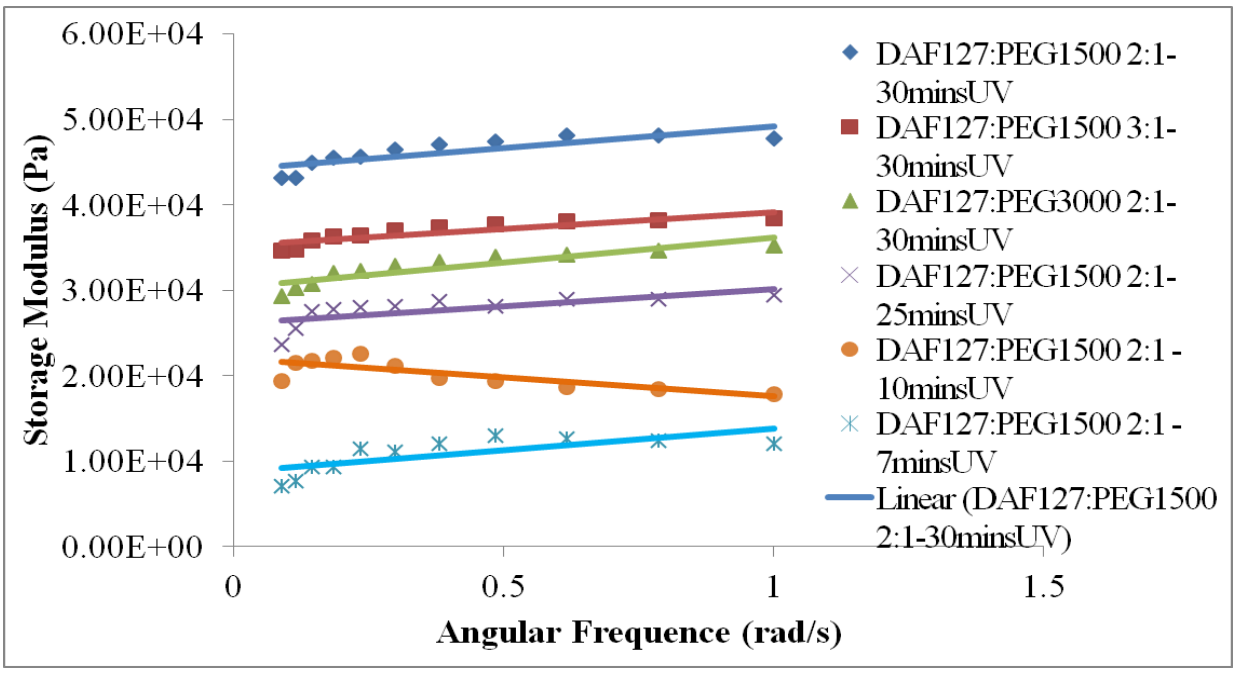

Figure 1.5: Comparison of storage modulus of Pluronics based hydrogel with different compositions and different UV irradiation times. DAF127 stands for diacrylated Pluronics F127, PEG1500 stands for PEG with an average molecular weight of 1500 Da and PEG3000 stands for PEG with an average molecular weight of 3000 Da. Due to error limits of the Anton Paar Physica MCR 301 rheometer, the curves of some samples were not smooth.

Table 1.1: Changes in weight of Pluronics based hydrogels in PBS for 10 days

Day	Weight of The Hydrogel (g)
0	0.56
1	1.12
2	1.12
3	1.13
4	1.14
7	1.17
9	1.19
10	1.19

The weight of the hydrogel was almost doubled during the first day of swelling, and the hydrogel reached an equilibrium value in about 10 days.

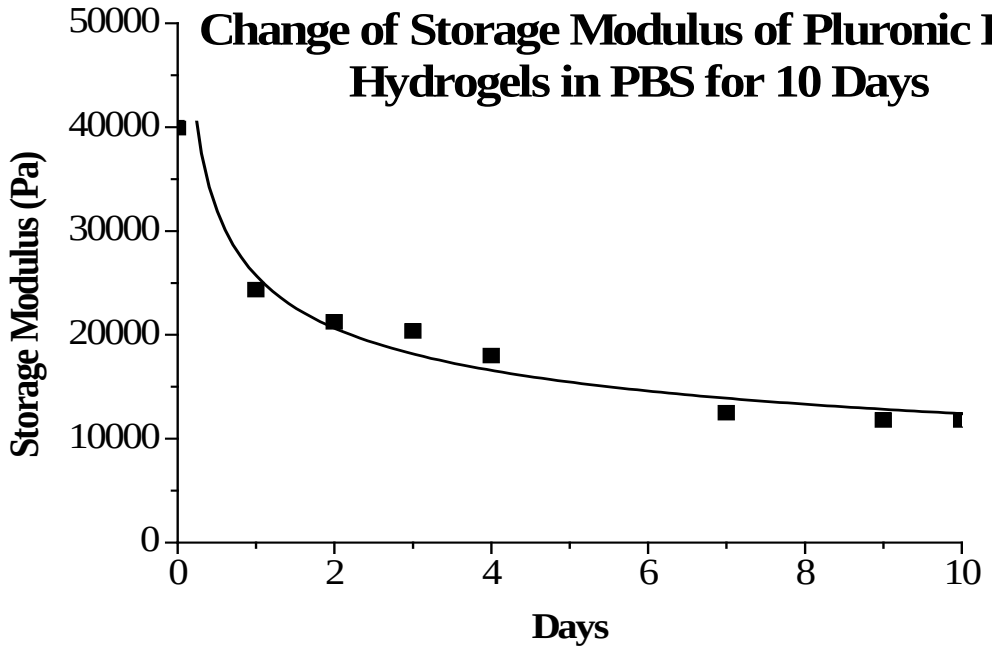

Figure 1.6: Changes of storage modulus of Pluronics based hydrogels in PBS for 10 days.

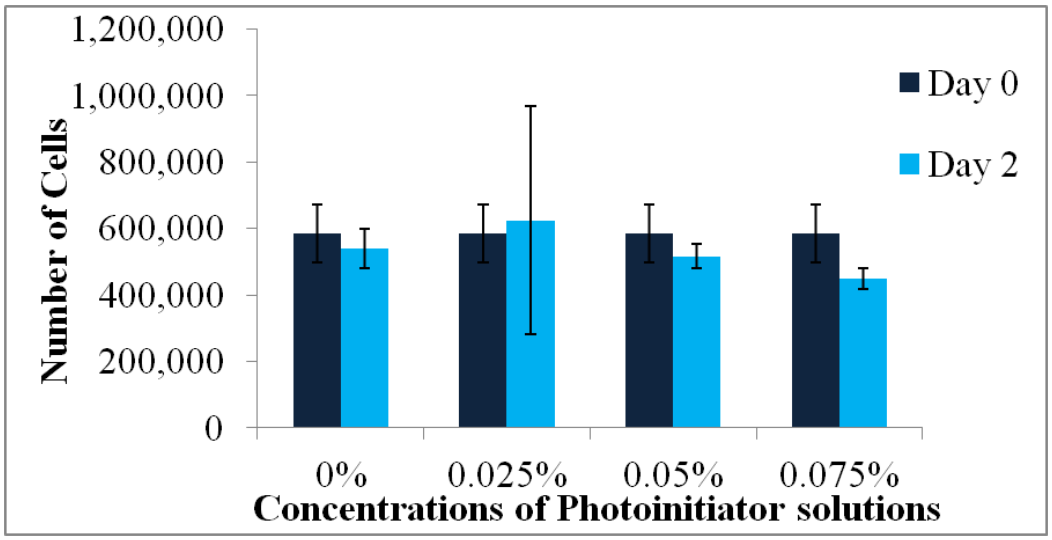

Figure 1.7: Cytotoxicity test of photoinitiator Irgacure 2959 on per-adipocyte. The number of cells on day 0 and day 2 were compared. The test was carried out in collaboration with Elluru. The design of the experiment and the preparation of the solution were performed by Guan while the measurements of cell number were carried out together with Elluru.

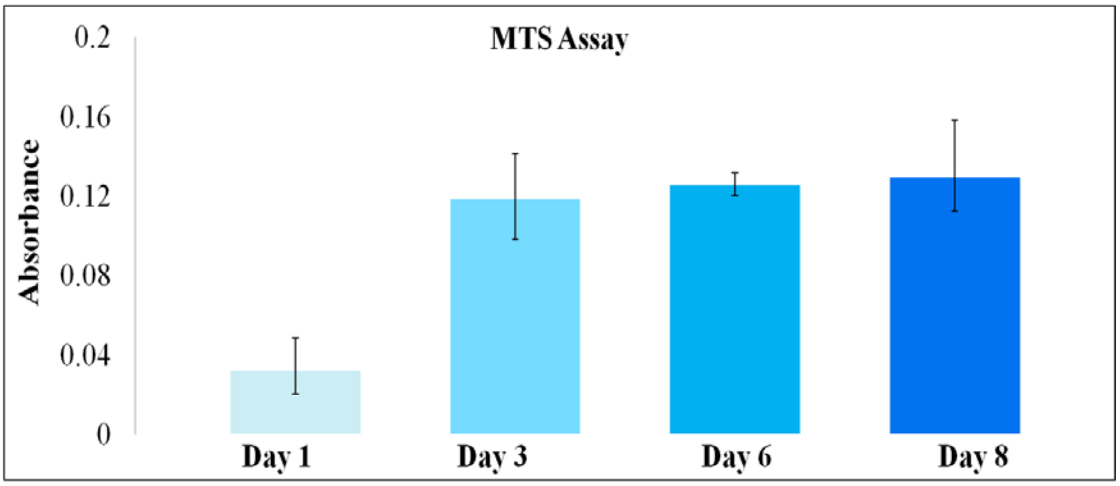

Figure 1.8: MTS Assay on pre-adipocyte culture, absorbance readings of day 1, 3, 6, 8 are compared. The test was carried out in collaboration with Elluru. The preparations of the solutions as well as the readings on day 6 were performed by Guan while the design of the experiment and the measurements on day 1, 3 and 8 were carried out together with Elluru.

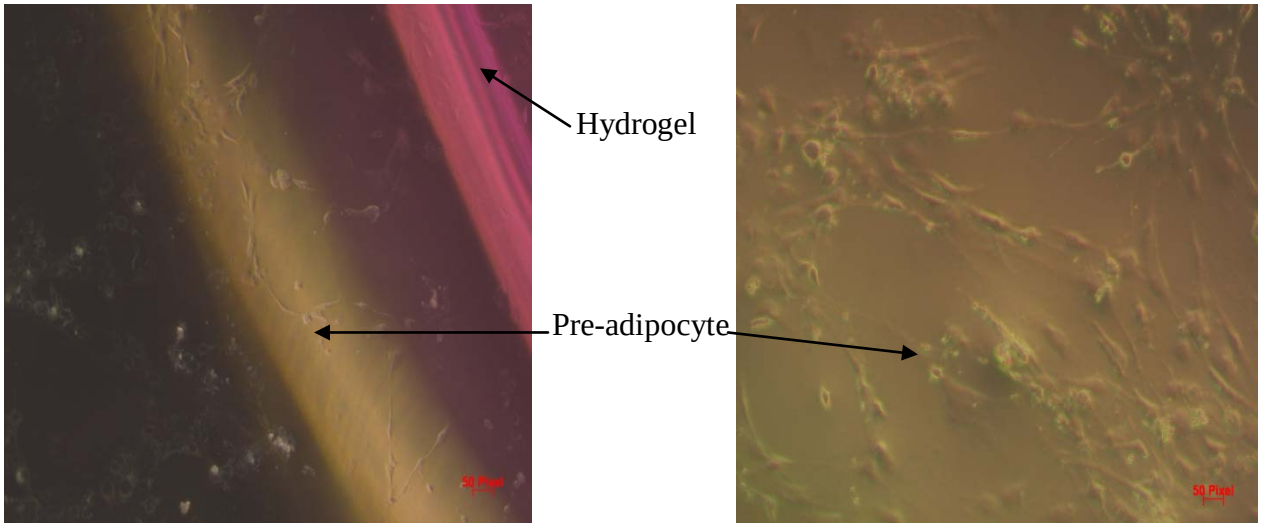

Figure 1.9: Phase contrast microscopy images of pre-adipocyte culture growth next to the Pluronics base hydrogel on day 3. The test was carried out in collaboration with Elluru. Preparations of hydrogels were performed by Guan while experimental design and phase contrast microscopy images were carried out in collaboration with Elluru.

Chapter II

1. Introduction

Clean water is essential to human health, agriculture, industry and the ecosphere. However, with the rapid development of industries, such as metal plating facilities, mining operations, and fertilizer industries, heavy metal pollution has become one of the most serious environmental problems today. Heavy metals are not biodegradable and tend to accumulate in living organisms. Many heavy metal ions are known to be toxic or/and carcinogenic. Toxic heavy metals of particular concern in treatment of industrial wastewater include zinc, copper, nickel, mercury, cadmium, lead and chromium. In order to tackle this pollution problem, the technology of removing heave metals from industrial and commercial waste water becomes relevant. Many methods and procedures, including chemical treatment, physical treatment, biological treatment, have been adopted to resolve this environmental problem.[1-7] Activated carbon adsorbents are widely used in the removal of heavy metal contaminants. However, the depleted source of commercial coal-based activated carbon results in a substantial increase in price.[1, 8-9] Therefore, a low cost, high efficiency and safe treatment of heavy metals is in great demand.

Electrospinning is a method of polymer fabrication technique that can create web-like non-woven nanofibrous membranes. Since these membranes have up to 40 m^2/g effective surface area and close to 80% effective porosity with continuously interconnected pores, they have many advantages in applications to water purification, such as microfiltration.[10] Microfiltration is a filtration process that removes contaminants from a fluid by passage through a microporous membrane with the pore sizes ranging from 0.1 to 10 μm.[11] However, as the pore sizes are much larger than those of dissolved metal ions in the form of hydrated ions, microfiltration membranes cannot be simply used for filtering heavy metal ions from an aqueous solution.[12-14]

Polysaccharides are among the most abundant natural polymers on earth, and cellulose is the simplest and most abundant one. As a major constituent of all plant matter, cellulose is relatively low cost.[15] In order to improve the removal efficiency of metal ions, a novel microfiltration membrane consisting of cellulose nanofibers (CNF) and amino modified cellulose nanofibers (mCNF) infused in an electrospun polyacrylonitrile (PAN) scaffold on a non-woven polyethylene terephthalate (PET) support was investigated.

Lead (II) is an example for positive charged metals in this study. The maximum limit concentration of lead (II) in drinking water is 0.015 mg/L.[16] Lead is a common metal found throughout the environment in lead-based paint, air, soil, dust, food, porcelain, pewter, and water. Lead can cause damage to the brain, red blood cells, and kidneys if too much of it enters one's body and builds up in the body over many years. Lead in drinking water, although rarely the sole cause of lead poisoning, can significantly increase a person's total lead exposure.[17] The Lead exists as lead ion (Pb^{2+}) in an acid solution and starts to precipitate at pH values higher than 6.5, depending on the concentration of lead ions (Figure 2.1).[18] In order to attract the positively charged lead ions, negatively charged cellulose nanofibers were produced. Isogai and his coworkers successfully prepared the ultra-fine cellulose nanofibers with diameters of about 5 nm and lengths of about 1 μm by the TEMPO oxidation method[19-21]. The cellulose nanofibers have large surface area and significant amounts of C6 carboxylate groups on the fiber surface, which can be modified for many applications.[19-21] In this case, the positively charged Pb^{2+} ions can be attracted by the negatively charged COO^- on the surface of CNF through electrostatic interactions.

Chromium (VI) is an example for negatively charged metal ions in this study. The maximum limit concentration of chromium (VI) in drinking water is 0.05 mg/L. Chromium (VI) has been

used for chrome plating, dyes and pigments, leather tanning, and wood preservation[22]. Breathing high levels of chromium (VI) can damage to the nose and cause cancer [22]. Further, ingesting high levels of chromium (VI) may result in anemia or damage to the stomach or intestines.[22] The hexavalent species of chromium exists primarily as chromic acid (H_2CrO_4), hydrogen chromate ion ($HCrO_4^-$) and chromate ion (CrO_4^{2-}), depending on pH (Figure 2.2).[23] In order to attract the negative charged chromium ions, the CNF were further modified to generate positive charges on the surface of the nanofibers. The CNF were amino-modified by polyvinylamine (PVAm) according to EDC reaction and the amino groups on the PVAm chains formed peptide bonds with the COO^- groups on the surface of the CNF. The abundant amino side chains of PVAm not only increased the efficiency of grafting, but also introduced enormous of amino group on the surface of mCNF. Therefore, the mCNF with positive surface charged were generated. In this case, the negative charged $HCrO_4^-$ and CrO_4^{2-} ions can be attracted by the positive charged amino groups ($-NH_3^+$) on the surface of mCNF through electrostatic interactions.

2. Experimental

2.1 Materials

Polyacrylonitrile (PAN) with an average molecular weight of 1.5×10^5 g/mol was purchased from Scientific Polymer Products. 98% N,N-dimethylformamide (DMF), N-(3-Dimethylaminopropyl)-N'-ethylcarbodiimide hydrochloride (EDC), N-Hydroxysuccinimide (NHS), 2,2,6,6-tetramethylpiperidine-1-oxylradical (TEMPO), sodium hypochlorite (NaClO), potassium chromate (K_2CrO_4), Lead (II) nitrate ($Pb(NO_3)_2$), sodium bromide (NaBr), 4-(2-pyridylaxo resorcinol) (PAR) and 1,5-Diphenylcarbzid were purchased from Sigma-Aldrich. The PET non-woven support was purchased from Sanko, Japan. Wood pulp (Biofloc 96 MV, Tembec

Tartas Factory in France) was selected as the source to produce ultra-fine cellulose nanofibers. 30% polyvinylamine (PVAm) solution was obtained BASF.

2.2 Electrospinning of PAN nanofibrous membrane

6 wt% of PAN solution was prepared by dissolving the PAN powder in DMF and stirring at 60 ºC until the solution was homogeneous, which might take around 24 hours. The solution was electrospun directly onto a PET substrate by using a computer-controlled electrospinning instrument, consisting of a metallic spinneret, a syringe pump, a high-voltage power supply, and a step-moving collector. The electrospinning instrument was operated in a closed environmental chamber, with the humidity adjusted by a compressed air flush system. Teflon tubing was used to connect the syringe pump to the spinneret for delivery of the PAN solution under controlled conditions. The sample was electrospun at a spinneret diameter of 1.0 mm, a solution flow rate of 25 μL/min, ambient temperature of 22 ºC, humidity of 50 %, a tip-to-collector distance of 10 cm and applied voltages between 13 to 15 kV. After the desired thickness of the PAN membranes were produced, the PAN membranes were taken out from the rotating drum collector and dried at room temperature for 24 hours prior to use or/and any further modifications. The electrospun PAN membranes were prepared with the help of graduate student Ran Wang.

2.3 Preparation of modified cellulose nanofibers

The procedure for the preparation of CNF and mCNF is shown in Figure 2.3. The CNF were prepared according to the procedure of TEMPO oxidation published earlier.[19-21] In short, wood pulp which contained 10 g dry weight of cellulose was dispersed in 100 g of water. Then, 2 g of

sodium bromide and 0.2 g of TEMPO agent were added into the suspension and stirred until all the powder materials were dissolved. To start the reaction, 75 g of 13% NaClO solution were added into the cellulose mixture, and the pH value of the mixture was controlled at 10-11 by adding 0.5 M NaOH solution. The mixture was stirred at room temperature for 24 hours. After the reaction was finished, the product was filtered and washed by distilled water several times to remove the extra salts, and the carboxylated ultra-fine cellulose nanofibers (CNF) with diameters of around 5 nm were achieved after ultrasonification. In order to produce amino-modified cellulose nanofibers (mCNF), the carboxylated cellulose nanofibers were grafted by PVAm using EDC and NHS as catalysts. To 100 ml of the carboxylated cellulose nanofibers suspension with 0.4% solid content, 6.7 g of PVAm solution, 0.1 g EDC and 0.07 g NHS were added, and the pH value was controlled at 7.5 – 8. After the mixture being stirred overnight at room temperature, the product was centrifuged and washed by distilled water several times to remove the excess reagents. Ultrasonification was applied on the product to generated mCNF suspension in desire concentrations.

2.4 Preparation of composite nanofibrous membrane

CNFs were used as testing adsorbents for Pb (II), while mCNFs were used as testing adsorbents for Cr (VI). In order to adapt microfiltration membranes for heavy metal adsorption, 4 ml of 0.01 wt% CNF/ mCNF suspension were infused into in a 2 inch diameter PAN scaffold on a non-woven PET support with an applied pressure of 2 psi. The concentrations of CNF/mCNF in the initial suspension and the permeate suspension were tested by using a total organic carbon analyzer (TOC-5000, Shimazu Corp). According to calculation, the density of CNF/mCNF in the PAN scaffold reached 0.05 mg/cm^2. These microfiltration membranes consisting of CNF/mCNF

infused in a PAN scaffold on a non-woven PET support were used for dynamic adsorption experiments. However, since the static adsorption does not require a membrane with strong mechanical strength, the PET support was peeled off from the membranes used in static adsorption experiments.

2.5 Characterizations of functional cellulose nanofibers

After the TEMPO oxidation, the carboxyl content of the CNF was determined by conductivity titration with 0.04 M NaOH solution. Freeze dried cellulose samples were scanned with a Thermo Scientific FTIR model Nicolet IS10. Infrared spectra of wood pulp, CNF and mCNF were recorded and analyzed for the newly introduced functional groups.

2.6 Composite membrane geometry

The morphology of membranes was detected by the scanning electron microscope (SEM, PEI Phenom) equipped with a Schottky field emission gun (10 kV) and a Robinson backscatter detector. All samples were coated by gold for a period of 30 seconds before scanning. The cross-sectioned samples were prepared by fracturing water-wetted membrane in liquid nitrogen. The fiber diameters and the cellulose nanofibrous barrier layer thickness were determined by using the SEM image together with a modified LeiKa software which was developed at Stony Brook (www.dell.chem.sunysb.edu).

2.7 Composite membrane porometry examination

The pore sizes of electrospun PAN scaffold, the CNF-PAN composite membrane and the mCNF-PAN composite membrane were determined by a capillary flow porometer (CFP-1500A from PMI porous material, INC). The Galwick wetting fluid was used for bubble point tests.

2.8 Static adsorption of heavy metal ions

Static adsorption experiments were carried out using the batch equilibration technique. The 1000 ppm stock solution for Pb (II) was prepared from Lead (II) nitrate ($Pb(NO_3)_2$), and the 1000 ppm stock solution for Cr (VI) was prepared from potassium chromate (K_2CrO_4). For static adsorption experiments, initial concentrations of metal solutions were prepared in the range 10-100 ppm by diluting the stock metal solutions. The pH values of the metal solutions were adjusted by adding negligible amounts NaOH and HCl solutions. A series of 50-ml centrifuge tubes containing 0.5-1 mg adsorbents and 5-10 ml solution were capped at room temperature until equilibrium was obtained. Since the adsorbents CNF/mCNF were infused into the PAN scaffold, they can be removed by taking out the membrane from the metal solution after the adsorption equilibrium has reached. In order to get an accurate measurement of the adsorption efficiency of the CNF/mCNF, static adsorption tests for both metals were also performed on the PAN scaffolds without any infusion of CNF/mCNF. The experiments were performed over a period of 24 hours, and the adsorption efficiencies were tested at different time points to find out the time duration needed for the adsorption. In order to learn about the pH effect on adsorption, the pH values of initial metal ion solutions were adjusted over a range of 2 – 6 for Pb (II) and 1 - 13for Cr (VI).The adsorption efficiencies at different pH values were compared to determine the optimal pH value. For the adsorption capacity experiments, different initial concentration of

metal ion solutions were treated with same amount of adsorbents, and adsorption capacity was calculated from the adsorption efficiency at different concentrations.

2.9 Dynamic adsorption of heavy metal ions

Dynamic adsorption experiments were carried out in an open-ended cell. Initial concentrations of metal solutions were prepared in 50 ppm, and the pH values of the metal solutions were adjusted by adding negligible amounts NaOH and HCl solutions. For each test, a volume of 50 ml metal solution was filtrated through a 2 inch diameter CNF/mCNF composite membrane by using a syringe at a speed of 2 ml/min. The metal solutions permeated for each experiment were collected in 5 portions, 10 ml each, and the adsorptions of each portion were tested. Dynamic adsorption tests for both metals were also performed on the PAN scaffolds without any infusion of CNF/mCNF in order to confirm that there was no removal of metals by the PAN scaffold itself. The adsorption efficiency (Q) for both static and dynamic adsorption was calculated as follows:

$$Q = V(Ci - Cf)/M_a \qquad (1)$$

where V was the volume of the metal ion solutions, M_a was the mass of the corresponding adsorbents, Ci and Cf were the metal ion concentrations of initial and after adsorption, respectively.

2.10 Desorption of heavy metal ions

After dynamic adsorption experiments were conducted, the 2 inch diameter CNF/mCNF composite membranes with metal ions attracted were dried and saved for desorption tests. Desorption experiments were carried out in a similar way as dynamic adsorption. The composite membrane was placed in an open-ended cell, and 5-ml of NaOH and HCl solution was filtrated through the membrane by using a syringe at a speed of 2 ml/min. The NaOH and HCl solutions permeated for each experiment were collected, and the metal concentrations of the solutions were tested. The desorption efficiency (*D*) was calculated as follows:

$$D\ (\%) = CdV / QM_a \qquad (2)$$

where V was the volume of the desorption metal ion solutions, M_a was the mass of the corresponding adsorbents, Cd was the metal ion concentrations of desorption, and Q was the adsorption efficiency of the membranes. All adsorption and desorption experiments were carried out at room temperature and duplicated three to five times.

2.11 Spectrophotometric determination of metals ions

The metal concentrations were measured by the UV-visible spectrophotometric method. The spectrophotometric method is highly sensitive to the metal concentration via complex formation with a chromogenic reagent in an aqueous solution. For measurements of Pb (II) concentration, 0.5 ml of 0-80 ppm Pb (II) solution was put into series of 10 ml volumetric flasks to which 0.6 ml of 0.024% (wt/v) PAR were added, and the borax buffer with pH equal to 9 was added to make up a volume of 10 ml. The maximum absorbance wavelength for the Pb-PAR complex was determined at 523 nm. For measurements of Cr (VI) concentration, 0.5 ml of 0-100 ppm Cr (VI)

solution was put into series of 10 ml volumetric flasks to which 0.5 ml of 0.25% (wt/v) 1,5-Diphenylcarbzid were added, and 0.5 N H_2SO_4 solution was added to make up a volume of 10 ml. The maximum absorbance wavelength for the complex was determined at 541 nm.

3. Results and Discussion

3.1 Functional groups in cellulose nanofibers

According to the result of conductivity titration, the amount of C6 carboxylate groups generated on the surface of the CNF was 2.08 ± 0.12 mmol/g. The introduced carboxyl groups will function as negatively charged domains for adsorption of positively charged metal ions. The additional characteristic peaks in the infrared spectra of the difference cellulose samples are shown in Figure 2.4.

The C=O stretching of the N-acetyl groups at 1680 cm^{-1} and the broad band for N-H vibration between 3000 cm^{-1} and 3300 cm^{-1} were evidence of the effective PVAm grafting of cellulose nanofibers and the formation of mCNF. The introduced amine groups will function as positively charged domains for adsorption of negatively charged metal ions.

3.2 Structure characterization of composite membrane

The PET non-woven membrane was chosen as the support for the electrospun PAN scaffold. Its mechanical properties were determined by the previous study, showing that it was the main load bearing component, responsible for the mechanical strength.[15] The average thickness of the PET support and the electrospun PAN scaffold are 104.4 ± 1.7 μm and 37.3 ± 6.4 μm, which were determined and confirmed by using a micrometer and a modified LeiKa software

developed at Stony Brook (www.dell.chem.sunysb.edu). The PET support had an average fiber diameter of (1.93 ± 0.89) x 10^4 nm which was about 100 times larger than that of the electrospun PAN scaffold (220 ± 50 nm). SEM microscopy images (Figure 2.5) showed that the electrospun PAN fibers were randomly deposited on the PET support, and formed a highly porous scaffold with a porosity of about 80% which was calculated by the weighing method. From the images of CNF/mCNF infused PAN membranes, the PAN fibers were intertwining by the cross-linked CNF/mCNF networks while the geometry of the electrospun membrane remained constant, and the porosity remained close to 80%.

3.3 Porometry examination of composite membrane

After the infusion of CNF/mCNF, the maximum pore size of PAN-PET membrane remained the same, but the mean flow pore size and pure water flux was reduced (Table 2.1). Although the mean flow pore size was reduced to 0.32 μm, it was still within the range of microfiltration. Also, the pure water permeability could be maintained at a higher value than that of ultrafiltration membranes which was about 100 L/m^2 h.psi. Since the mean flow pore size of the composite membrane was much larger than the size of dissolved metal ions in the hydrated form, the composite membrane could be used to remove metal ions by electrostatic interactions, not by size exclusion.

3.4 Time influence on adsorption

For adsorption of Pb (II), 0.7 mg of adsorbents were added into 10 ml Pb (II) solution with an initial concentration of 50 ppm, and the pH value of the solution was adjusted to 6 by adding a

negligible amount NaOH solution. For adsorption of Cr (VI), 1.2 mg of adsorbents were added into 40 ml Cr (VI) solution with an initial concentration of 15 ppm, and the pH value of the solution was adjusted to 4 by adding a negligible amount of HCl solution. The static adsorption tests on the PAN scaffold confirmed that it had negligible adsorption or rejection for both metal ions. Therefore, only the weights of CNF and mCNF were considered as adsorbents in this study. Table 2.2 lists the influence of time on metal adsorptions which were carried out at room temperature. For the Pb (II) experiment, the adsorption increase slowly during the first 4 hours, and almost stopped increasing after 24 hours. In contrast, it is clear that the adsorption increase rapidly during the first 1hour for the Cr (VI) experiment, but it did not change much after that. Thus, for the adsorptions of Pb (II) and Cr (VI), a period of 24 hours could be considered to have essentially reached the equilibration state.

3.5 Solution pH influence on adsorption of Pb (II) and Cr (VI)

For the Pb (II) experiments, 0.7 mg of adsorbents were added into 10 ml Pb (II) solution with an initial concentration of 50 ppm, and the pH of the solution was adjusted by adding negligible amounts of HCl solution and NaOH solution to the range of 2-6. The reason why the pH of Pb (II) solution was not adjusted to below 2 was because most of the carboxyl groups on the surface of the CNF would be protonated at low pH values and thereby lost their ability to attract the Pb (II) ions. Furthermore, due to formation of white precipitate of Lead (II) hydroxide ($Pb(OH)_2$) around pH 6.5, the pH of the Pb (II) solution was not adjusted to above 6. The experiments were conducted at room temperatures for 24 hours before taking the UV readings.

Figure 2.6 shows the pH influence on the adsorption of Pb (II). The adsorption of Pb (II) increased with increasing pH value from 2 to 6 and reached a maximum at pH 6. This was due to the influence of pH on the protonation of carboxyl groups on the surfaces of CNF. As the pH value was increased from 2 to 6, the carboxyl groups on the surface of CNF started to deprotonate and changed from no charge to negative 1 charge. As the number of deprotonated carboxyl groups increased, the ability of the CNF to attract the Pb (II) ions increased. At the same time, the Pb (II) remained as positive 2 charged ions in this pH range. Therefore, the experiment indicated that the solution pH could affect the adsorption of Pb (II) by CNF, and the optimum pH for adsorption was 6. Since the original pH value of the Lead (II) nitrate solution was in the range of 4.7 to 5.2 in the concentration range between 1000 to 10 ppm, it did not require us using too much NaOH solution to adjust the pH to 6. Therefore, it was convenient and beneficial to adjust the Pb (II) solution to pH 6 in order to optimize the adsorption condition.

For the Cr (VI) experiment, 0.5 mg of adsorbents were added into 10 ml Cr (VI) solution of an initial concentration of 15 ppm, and the pH of the solution was adjusted by adding negligible amounts of HCl solution and NaOH solution to the range of 1 to 13. The experiments were conducted at room temperature for 24 hours before taking the UV readings.

Figure 2.6 also shows the pH influence on the adsorption of Cr (VI). The adsorption of Cr (VI) increased with increasing pH value from 1 to 4 and reached a maximum at pH = 4. However, the adsorption decreased with increasing pH from 4 to 13. This was due to the influence of pH on the Cr (VI) species in the solution and the protonation of amino groups on the surfaces of mCNF. As the pH value was increased from 1 to 4, the primary species of Cr (VI) changed from no charge in H_2CrO_4 to the charged form $HCrO_4^-$. Therefore, the $HCrO_4^-$ species could be attracted by the positively charged amino groups ($-NH_3^+$) on the surface of mCNF

through electrostatic interactions. As pH increased from 4 to 13, the primary species of Cr (VI) changed from $HCrO_4^-$ to CrO_4^{2-}, and the charge changed from -1 to -2. In order to attract one Cr atom, the number of amino groups was increased from one to two. Also, as the pH value was increased from 1 to 13, the amino groups on the surface of mCNF started to deprotonate and lost the positive charge. As a result, the amino groups on the surface of mCNF then lost the ability to attract the Cr (VI) species. Thus, the adsorption of Cr (VI) decreased with increasing pH from 4 to 13. The experiment indicated that the solution pH could affect the adsorption of Cr (VI), and the optimum pH value for Cr (VI) adsorption was 4. Since the original pH value of the H_2CrO_4 solution was in the range of 4.08 to 4.8 in the concentration between 1000 to 10 ppm, little HCl solution was needed to adjust the pH value to 4. It is convenient and beneficial to adjust the Cr (VI) solution to pH = 4 to optimize the adsorption condition. In practice, the pH value of those pollutants should be adjusted to the optimal pH value, as shown in Figure 2.6, in order to take advantage of the maximal adsorption capacity of the membrane.

3.6 Adsorption isotherms of Pb (II) and Cr (VI)

For the Pb (II) experiment, 0.7 mg of adsorbents were added into 10 ml Cr (VI) solution with an initial concentration varying from 10 – 80 ppm, and the pH value of the solution was adjusted to 6 by adding negligible amounts of NaOH solution. The higher concentration of Pb (II) had not been tested due to the precipitation of $Pb(OH)_2$. The higher the concentration of Pb (II), the lower the pH value of the precipitation which was close to 6. The experiments were conducted at room temperature for 100 hours before taking the UV readings.

Figure 2.7 shows the adsorption isotherms of Pb (II). As the initial concentration of Pb (II) solution increased from 10 to 50 ppm, the amount of Pb (II) adsorbed at equilibrium was also increased. However, as the initial concentration of Pb (II) solution was exceeding 50 ppm and was increased to 80 ppm, the amount of Pb (II) adsorbed increased slowly and reached a maximum. The Pb (II) adsorption isotherms of CNF could be fitted well to the Langmiur model

$$\frac{Ce}{Qe} = \frac{Ce}{Qm} + \frac{1}{K_L Q_m} \tag{3}$$

where Ce stands for the equilibrium concentration, Qe stands for the adsorption at equilibrium, K_L is the constant related to the adsorption energy and Qm is the saturated adsorption. In order to find out the value of Qm, Ce/Qe is plotted against Ce (Figure 2.8). The data fit well linearly. Qm = 159 mg/g, based on the slope of the linear line.

For the Cr (VI) experiment, 1 mg of adsorbent was added into 5 ml Cr (VI) solution with initial concentrations varying from 15 – 100 ppm. The pH value of the solution was adjusted to 4 by adding HCl solution. The experiments were conducted at room temperature for 100 hours before taking the UV readings.

Figure 2.9 shows the adsorption isotherms of Cr (VI). As the initial concentration of Cr (VI) solution increased from 15 to about 50 ppm, the amount of Cr (VI) adsorbed at equilibrium was also increased. However, as the initial concentration of Cr (VI) solution exceeded 50 ppm, the amount of Cr (VI) adsorbed increased slightly and reached a maximum. The Cr (VI) adsorption isotherms of mCNF could be fitted well according to the Langmiur model Qm = 71 mg/g (Figure 2.10).

3.7 Dynamic adsorption of Pb (II) and Cr (VI)

For the Pb (II) experiment, 50 ml of 50 ppm Pb solution with pH value adjusted to 6 was filtered through a 2 inch diameter CNF composite membrane. Figure 2.11 shows the dynamic adsorption of Pb (II). The highest adsorption was obtained at the first 10 ml Pb (II) solution. Then, as the amount of Pb (II) solution passed through the membrane was increased, the adsorption efficiency was decreased. When the fifth 10 ml Pb (II) solution was filtrated out from the CNF composite membrane, there was almost no adsorption observed. Therefore, for the total of 50 ml of 50 ppm Pb (II) solution, the adsorption efficiency of Pb (II) on CNF was 259 mg.

For the Cr (VI) experiment, 50 ml of 50 ppm Cr (II) solution with the pH value adjusted to 4 was filtrated through a 2-inch diameter mCNF composite membrane. Figure 2.12 shows the dynamic adsorption of Cr (VI). Almost the same situation as Pb (II), the highest adsorption was obtained at the first 10 ml Cr (VI) solution. Then, as the amount of Cr (VI) solution passing through the membrane was increased, the adsorption efficiency was decreased. When the fifth 10 ml Cr (VI) solution was filtrated out form the mCNF composite membrane, there was almost no adsorption observed. Therefore, for the total of 50 ml of 50 ppm Cr (VI) solution, the adsorption efficiency of Cr (VI) on mCNF was 100 mg.

For both of Pb (II) and Cr (VI), the saturation capacities for dynamic adsorption of the CNF/mCNF composite membranes were higher than those for the static adsorption. This may due to the adsorption being occurred first in the middle of the CNF/mCNF composite membranes. As the SEM images showed, the PAN scaffold of the CNF/mCNF composite membrane could be contributed by many electorspun nanofibers randomly deposited on the PET support to make up a thickness of 37.3 μm. After the infusion, the CNF/mCNF penetrated into the 37.3 μm thick PAN scaffold and intertwined with the electorspun PAN nanofibers while

retaining a porosity of close to 80 % in the composite membrane. For dynamic adsorption, as the metal-containing solution was passing through the composite membrane which was filled with absorbents, the metals could be removed effectively. However, the metal solution could only contact the surfaces of the CNF/mCNF composite membranes in the static adsorption, and the adsorption efficiency was limited. Therefore, the proper thickness of the PAN scaffold could affect the adsorption efficiency, which was maximized in the dynamic adsorption.

3.8 Desorption of Pb (II) and Cr (VI)

From the study of the pH effect on Pb (II) adsorption, very little adsorption could be obtained from a metal solution with pH lower than 2. Therefore, 1 M HCl solution was used to treat the CNF composite membrane for desorption. On the other hand, 0.1 M NaOH solution was selected to treat the mCNF composite membrane for desorption, since there was little adsorption obtained from a metal solution with pH higher than 13 from the study of the pH influence on Cr (VI) adsorption. Based on the above observation, the metal ions on the composite membrane could be removed close to 100 % removed by using HCl and NaOH solutions for both cases. More importantly, followed by a wash with distilled water, the composite membrane could be recycled and reused.

3.9 Comparison of reported static adsorption capacities of Pb (II) and Cr (VI)

The adsorption capacities of Pb (II) and of Cr (VI) in this study were compared to the reported results of some commercial activated carbon products (Table 2.3). When compared with the reported values of some commercial activated carbon products, the level of adsorption

capacity of Pb (II) by CNF was considered to be high. Although the adsorption capacity of Cr (VI) by mCNF was not as high as the one of Pb (II), it was close to those of the commercial products.

4. Conclusion

A novel microfiltration membrane consisting of CNF/mCNF infused in an electrospun PAN scaffold on a non-woven PET support was investigated. Although the pore size of the PAN-PET membrane was reduced after the infusion of CNF/mCNF, it was still within the range of microfiltration. The adsorption performance of the composite membrane was influenced by the pH value of the metal solution. For Pb (II), the saturation capacity of the CNF composite membrane was 159 mg/g Pb (II) by static adsorption and 259 mg/g Pb (II) by dynamic adsorption at an optimum pH value of 6. For Cr (II), the saturation capacity of the mCNF composite membrane was 71 mg/g Cr (VI) by static adsorption and 100 mg/g Cr (VI) by dynamic adsorption at an optimum pH value of 4. Also, 100 % of the metal ions could be removed from the composite membrane by desorption, and the composite membrane could be recycled and reused. Compare with commercial activated carbon products, the adsorption capacity of Pb (II) by CNF was superior, while the adsorption capacity of Cr (VI) by mCNF was comparable. Although there were only two heavy metal examples in this study, the adsorptions were not limited to Pb (II) and Cr (VI). The adsorption mechanisms of the composite membranes were charge specific. Thus, they could be used for other charged ion removal. Overall, a novel, low cost, safe and effective method for heavy metal removal has been developed to a promising initial stage. It should be interesting to study a composite membrane which has the ability to

remove both negatively charged ions and positively charged ions together. In order to do so, the nanofibers must have free negative and positive charges. Such a configuration is within our reach in the current set up.

References

1. Fu, F., Wang, Q. (2011). Removal of heavy metal ions form wastewaters: A review. *Journal of Environmental Management,* **92**(3), 407-418.
2. Swmi, Deepika., Buddhi, D. (2006). Removal of contaminants from industrial wastewater through various non-conventional technologies: A review, *International Journal of Environment and Pollution,* **27**(4), 324-346.
3. Cotman, M., Zagorc-Koncan, J., Drolc, A. (2001). Study of impacts of treated wastewater to the Krkariver. *Water Science &Technolog,* **44**(6): 47-54.
4. Dabrowski, A., Hubicki, Z., Podkoscielny, P., Robens, E. (2004). Selective removal of the heavy metal ions from waters and industrial wastewaters by ion-exchange method. *Chemosphere*, **56**(7): 91-106.
5. Taylor, P. (2006). Removal of trace concentrations of heavy metals using complexing ion-exchange resins. *Separation Science and Technology*,**41**(8): 2575-2579.
6. Waqner-Dobler, I., Canstein, V.H., Li, Y., Timmis, K. N., Deckwer, W. (2000). Removal of mercury from chemical wastewater by microorganisms in technical scale. *Environmental Science and Technology*, **34**(11): 4628-4634.
7. Diels, L., Spaans, P. H., Van Roy, S., Hooberghs, L., Rynqaert, A., Wouters, H., Walter, E., Winters, J., Macaskie, L., Finlay, J., Pernfuss, B., Woebking, H., Pumpel, T., Tsezos, M. (2003). Heavy metals removal by sand filters inoculated with metal sorbing and precipitating bacteria. *Hydrometallurgy*, **71**(10): 235-241
8. Jusoh, A., Shiung, L. S., Ali, N., Noor, M. J. M. M., (2007). A simulation study of the removal efficiency of granular activated carbon on cadmium and lead. *Desalination,* **206**: 9-166.
9. Kang, K. C., Kim, S. S., Choi, J. W., Kwon, S. H. (2008). Sorption of Cu^{2+} and Cd^{2+} onto acid- and base- pretreated granular activated carbon and activated carbon fiber samples. *Journal of Industrial and Engineering Chemistry*,**14**: 131-135.
10. Wang, R., Liu, Y.; Li, B., Hsiao, B. S., Chu, B. (2012). Electrospun nanofibrous membranes for high flux microfiltration. *Journal of Membrane Science, 392-393*, 167-174.
11. Yoon, K., Hsiao, B. S., Chu, B. (2009). High flux ultrafiltration nanofibrous membranes based on polyacrylonitrile electrospun scaffolds and crosslinked polyvinyl alcohol coating. *Journal of Membrane Science*, *338* (1-2), 145-152.
12. Yoon, Y., Yoon, J., Amy, G., Chung, J., Sohn, J. (2009). Removal of toxic ions (chromate, arsenate, and perchlorate) using reverse osmosis, nanofiltration, and ultrafiltration membranes. *Chemosphere, 77* (2), 228-235.
13. Benitez, F. J., Acero, J. L., Real, F. J., Garcia, C. (2009). Removal of phenyl-urea herbicides in ultrapure water by ultrafiltration and nanofiltration processes. *Water Research,43* (2), 267-276.

14. Yoon, K., Kim, K., Wang, X., Fang, D., Hsiao, B. S., Chu, B. (2006) High flux ultrafiltration membranes based on electrospun nanofiberous PAN scaffolds and chitosan coating. *Polymer, 47* (7), 2434-2441.
15. Fox, S. C., Li, B., Xu, D., Edgar, K. J. (2011). Regioselective esterification and etherification of cellulose: A review. *Biomacromolecules,12* (6), 1956-1972.
16. WHO (1993), Guidelines for Drinking-Water Quality (2nd ed.). Geneva, Switzerland:
17. United States Environmental Protection Agency (2002). Lead in drinking water regulation public education guidance. Darby, PA: DIANE Publishing
18. Machida, M., Kikuchi, Y., Aikawa, M., Tatsumoto, H. (2004). Kinetics of adsorption and desorption of Pb (II) in aqueous solution on activated carbon by two-site adsorption model. *Colloids and Surfaces A: PhysicochemicalandEngineeringAspects, 240*, 179-186.
19. Isogai, A., Saito, T., Fukuzumi, H. (2011). TEMPO-oxidized cellulose nanofibers. *Nanoscale, 3* (1), 71-85.
20. Isogai, A., Fukuzumi, H., Saito, T., Okita, Y. (2010). Thermal stabilization of TEMPO-oxidized cellulose. *Polymer Degradation and Stability, 95* (9), 1502-1508.
21. Isogai, A., Saito, T., Kimura, S., Nishiyama, Y. (2007). Cellulose nanofibers prepared by TEMPO-mediated oxidation of native cellulose. *Biomacromolecules, 8* (8), 2485-2491.
22. Agency for Toxic Substances and Disease Registry. (2008). Toxic Substances Portal - Chromium. Retrieved from http://www.atsdr.cdc.gov/toxfaqs/TF.asp?id=61&tid=17
23. Dionex (1996), Determination of Cr (VI) in water, wastewater and solid waste extracts, Technical Note 26 LPN 34398-01 1M 7/96, Dionex Corporation.
24. Ma, H., Yoon, K., Rong, L., Mao, Y., Mo, Z., Fang, D. (2010). Hollander, Z; Gaiteri, J.; Hsiao, B.; Chu, B., High-flux thin-film nanofibrous composite ultrafiltration membranes containing cellulose barrier layer. *Journal of Membrane Science*, *20* (22), 4692–4704.
25. Rivera-Utrilla, J., Bautista-Toledo, I., Ferro-Garcia, M. A., Moreno-Castilla, C. (2003). Bioadsorption of Pb (II), Cd (II), and Cr (VI) on activated carbon from aqueous solutions. *Carbon, 41*, 323-330.
26. Kadirvelu, K., Faur-Brasquet, C., Le Cloirec, P. (2000). Removal of Cu (II), Pb (II) and Ni (II) by adsorption onto activated carbon cloths. *Langmuir, 16*, 8404-8409.
27. Hu, Z., Lei, L., Li, Y., Ni, Y. (2003). Chromium adsorption on high-performance activated carbons from aqueous solution. *Separation Purification Technology, 31*, 13-18.

Appendices

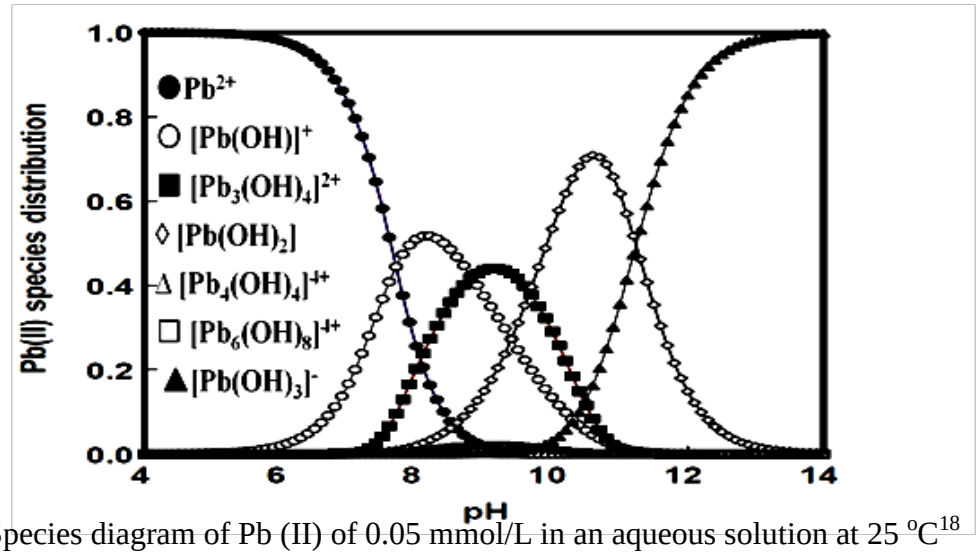

Figure 2.1: Species diagram of Pb (II) of 0.05 mmol/L in an aqueous solution at 25 ^{o}C[18]

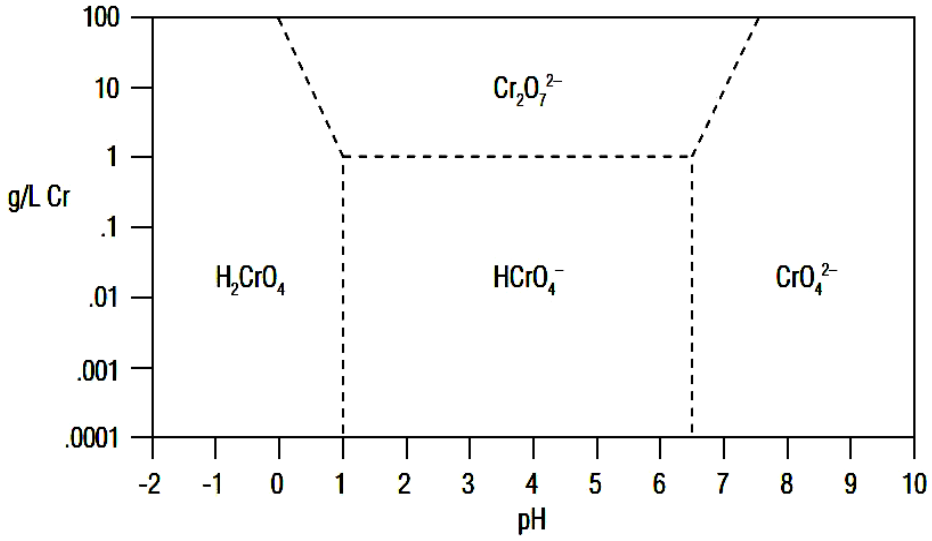

Figure 2.2: Relative distribution of Cr (VI) species in water as a function of pH and concentration.[23]

Equation 1

$$Q = V(Ci - Cf)/Ma \quad (1)$$

where Q was the adsorption efficiency, V was the volume of the metal ion solutions, Ma was the mass of the corresponding adsorbents, Ci and Cf were the metal ion concentrations of initial and after adsorption, respectively.

Equation 2

$$D (\%) = CdV / QMa \quad (2)$$

where D was the desorption efficiency, V was the volume of the desorption metal ion solutions, Ma was the mass of the corresponding adsorbents, Cd was the metal ion concentrations of desorption, and Q was the adsorption efficiency of the membranes.

Equation 3

$$\frac{Ce}{Qe} = \frac{Ce}{Qm} + \frac{1}{K_L Q_m} \quad (3)$$

where Ce stands for the equilibrium concentration, Qe stands for the adsorption at equilibrium, K_L is the constant related to the adsorption energy and Qm is the saturated adsorption.

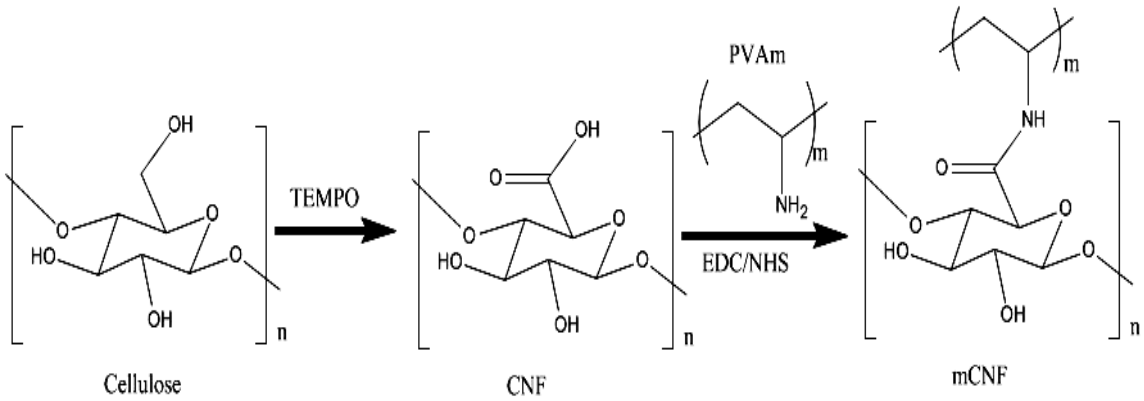

Figure 2.3: Oxidation and PVAm grafting of ultra-fine cellulose nanofibers.

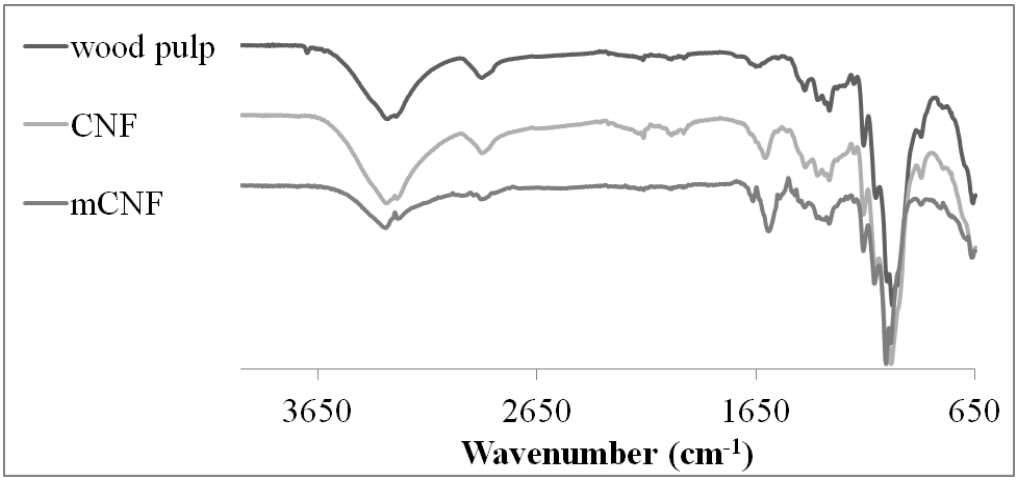

Figure 2.4: FTIR spectra of wood pulp, CNF and mCNF.

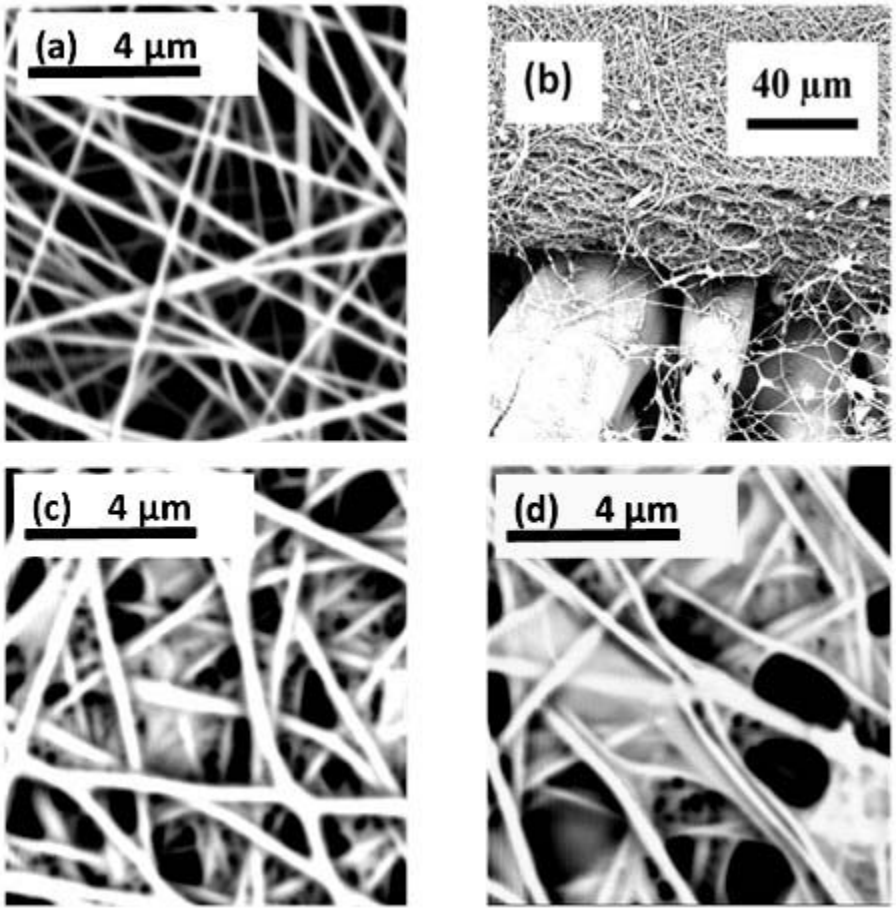

Figure 2.5: SEM microscopy images of PAN-PET membrane, CNF infused PAN-PET membrane and mCNF infused PAN-PET membrane: a. top view of PAN membrane; b. cross-sectioned of PAN-PET membrane[10]; c. top view of CNF infused PAN membrane; d. top view of mCNF infused PAN membrane.

Table 2.1: Structure of PAN-PET membrane, CNF infused PAN-PET composite membrane and mCNF infused PAN-PET composite membrane

Material	**PAN-PET**	**CNF-PAN-PET**	**mCNF-PAN-PET**
Maximum pore size (µm)	0.78	0.73	0.78
Mean flow pore size (µm)	0.66	0.38	0.32
Pure water flux (L/m^2 h.psi)	~3000	~1300	~1300

After the infusion of CNF/mCNF, the maximum pore size of PAN-PET membrane remained the same, but the mean flow pore size and pure water flux was reduced. Although the mean flow pore size was reduced to 0.32 µm, it was still within the range of microfiltration.

Table 2.2: Time influence on the adsorption of Pb (II) and Cr (VI)

Time	Pv (II) in mg adsorbed by CNF in g (mg/g)	Cr (VI) in mg adsorbed by mCNF in g (mg/g)
15 minutes	30.3 ± 3.6	46.1 ± 5.1
30 minutes	49.7 ± 3.3	48.0 ± 0.6
45 minutes	67.6 ± 7.9	53.1 ± 8.0
1 hour	75.6 ± 8.0	57.6 ± 1.1
2 hours	85.9 ± 3.3	60.1 ± 1.3
4 hours	107.3 ± 9.0	62.7 ± 6.1
24 hours	119.2 ± 10.3	63.0 ± 8.5

For the adsorptions of Pb (II) and Cr (VI), a period of 24 hours could be considered to have essentially reached the equilibration state.

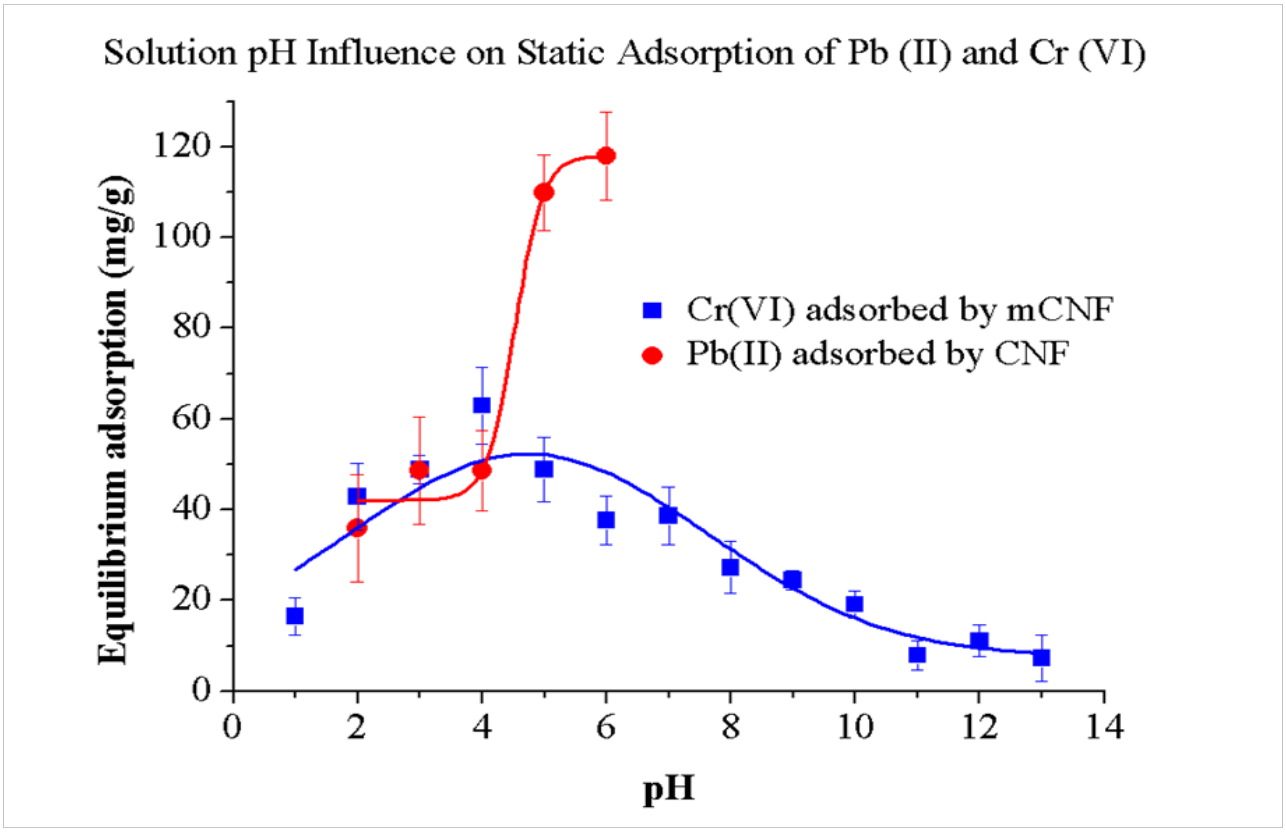

Figure 2.6: Solution pH influence on static adsorption of Pb (II) and Cr (VI).

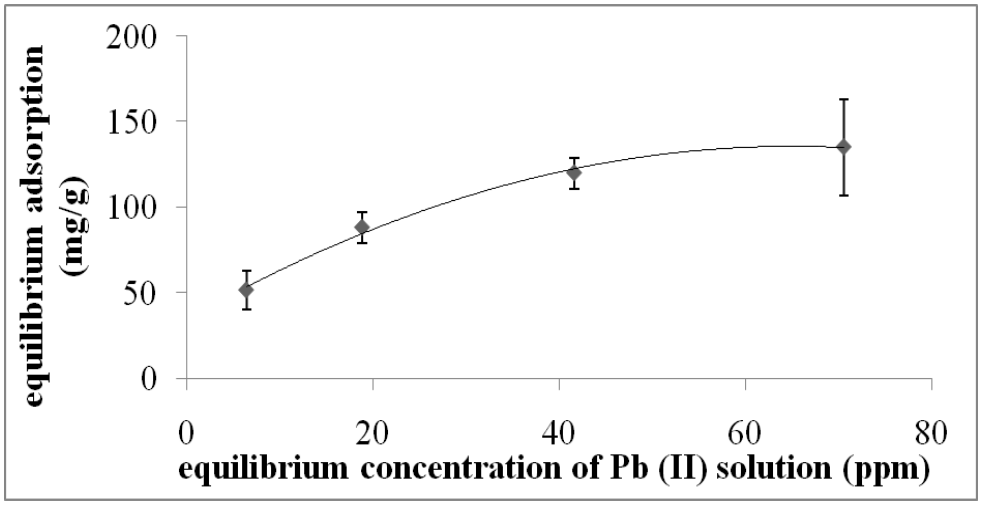

Figure 2.7: Adsorption isotherms of Pb (II) on CNF.

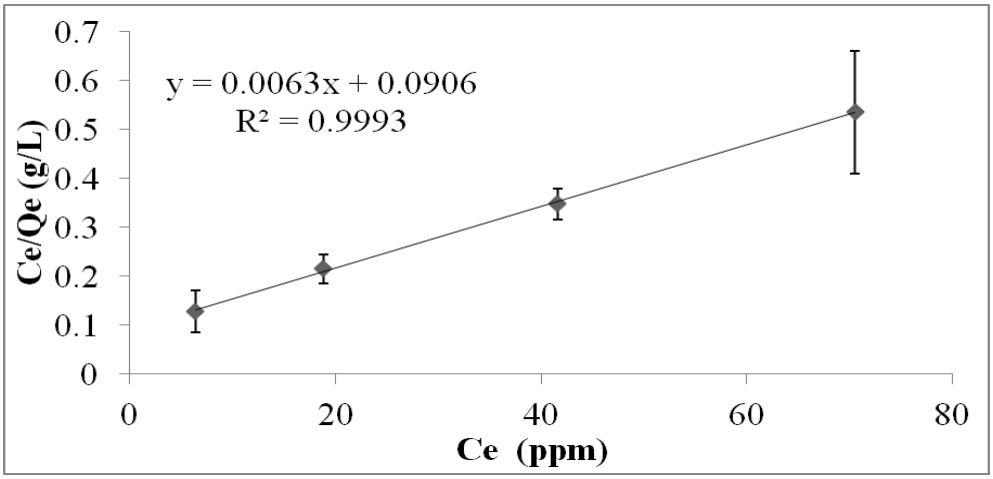

Figure 2.8: Langmuir model of Pb (II) adsorption isotherms.

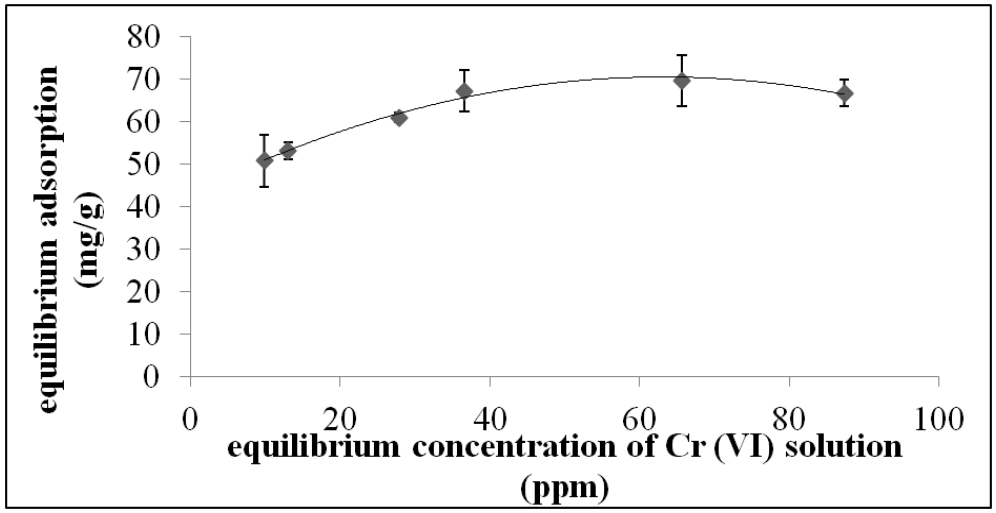

Figure 2.9: Adsorption isotherms of Cr (VI) on mCNF.

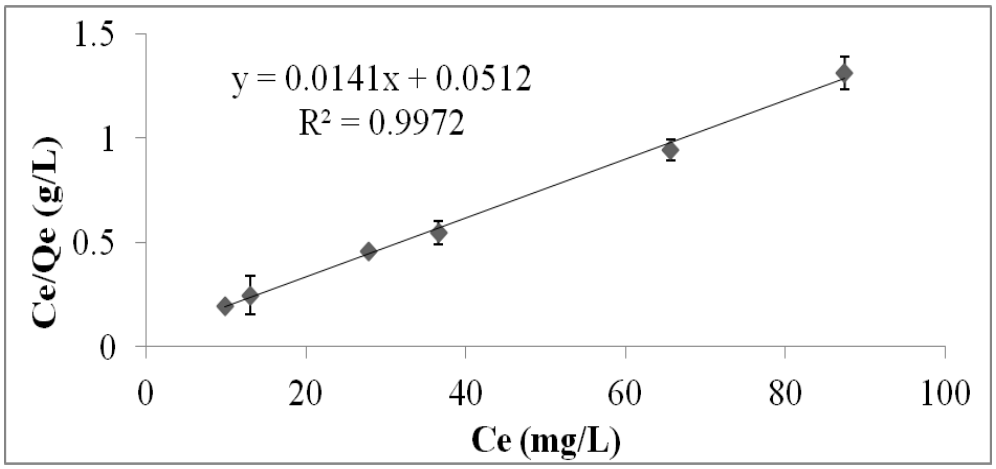

Figure 2.10: Langmuir model of Cr (VI) adsorption isotherms.

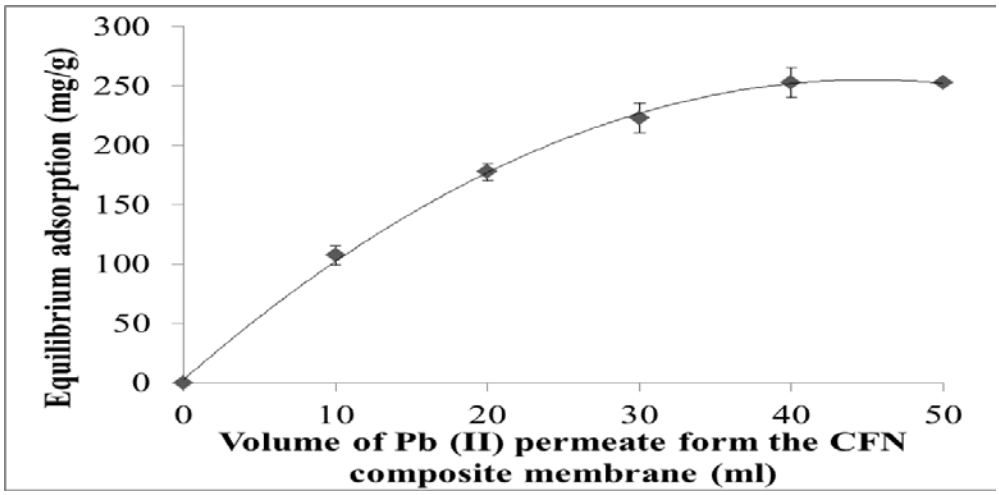

Figure 2.11: Dynamic adsorption of Pb (II) on CNF.

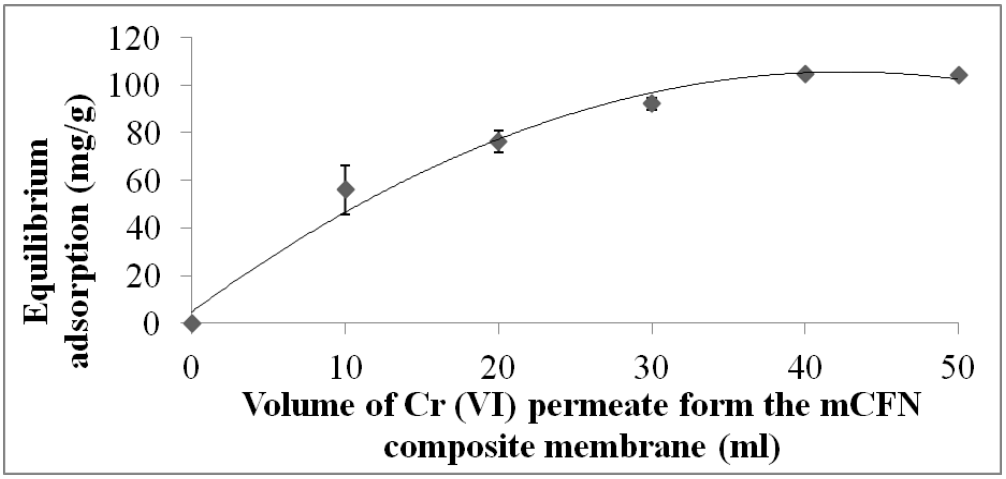

Figure 2.12: Dynamic adsorption of Cr (VI) on mCNF.

Table 2.3: Comparison of reported static adsorption capacities of Pb (II) and Cr (VI)

Type of adsorbent	Pb (II) Qm (mg/g)	Cr (VI) Qm (mg/g)
CNF	159 at pH=6	-
mCNF	-	71 at pH=4
Granular activated carbon of Merck brand (#102518)[25]	21.5 at pH =5.5	3.9 at pH=6.5
Activated carbon cloths CS 1501 (with 96% of micropore volume) from the Actitex Co.[26]	30.5 at pH ~3-4	-
Activated carbon cloths RS 1301 (with 32 % of mesopore volume) from the Actitex Co.[26]	25.7 at pH ~3-4	-
Granular activated carbon made form coconut shell (Calgon Mitsubishi Chemical Corporation, Diasorb W10-30)[18]	13.7 at pH ~5.4-6	-
Activated carbon FS-100 (Flitrasorb100, Calgon)[27]	-	69.3 at pH=3.2
Activated carbon SHT (Shanghai Cocking & Chemical Co. Ltd., China)[27]	-	69.1 at pH=3.2

When compared with the reported values of some commercial activated carbon products, the level of adsorption capacity of Pb (II) by CNF was considered to be high, and the adsorption capacity of Cr (VI) by mCNF was close to those of the commercial products.